

①

AD-A284 579



PL-TR-94-2035

**An Integrated Approach to Seismic Event Location:
II. Sources of Location Uncertainty for Teleseismic
and Local Network Data**

Cliff Frohlich

**Institute for Geophysics
University of Texas at Austin
8701 North Mopac Expressway
Austin, Texas 78759-8397**

14 February 1994

**Final Report
1 July 1991 through 28 February 1994**

**DTIC
ELECTE
AUG 25 1994
S G D**

Approved for public release; distribution unlimited

DTIC QUALITY INSPECTED 5



**PHILLIPS LABORATORY
Directorate of Geophysics
AIR FORCE MATERIEL COMMAND
HANSCOM AIR FORCE BASE, MA 01731-3010**


5905
94-27180



94 8 24 203

The views and conclusions contained in this document are those of the authors and should not be interpreted as representing the official policies, either express or implied, of the Air Force or the U.S. Government.

This technical report has been reviewed and is approved for publication.


KATHARINE KADINSKY-CADE
Contract Manager
Earth Sciences Division


JAMES F. LEWKOWICZ, Director
Earth Sciences Division

This report has been reviewed by the ESC Public Affairs Office (PA) and is releasable to the National Technical Information Service (NTIS).

Qualified requestors may obtain additional copies from the Defense Technical Information Center. All others should apply to the National Technical Information Service.

If your address has changed, or if you wish to be removed from the mailing list, or if the addressee is no longer employed by your organization, please notify PL/TSI, 29 Randolph Road, Hanscom AFB, MA 01731-3010. This will assist us in maintaining a current mailing list.

Do not return copies of this report unless contractual obligations or notices on a specific document requires that it be returned.

REPORT DOCUMENTATION PAGE			Form Approved OMB No. 0704-0188	
Public reporting burden for this collection of information is estimated to average 1 hour per response, including the time for reviewing instructions, searching existing data sources, gathering and maintaining the data needed, and completing and reviewing the collection of information. Send comments regarding this burden estimate or any other aspect of this collection of information, including suggestions for reducing this burden, to Washington Headquarters Services, Directorate for Information Operations and Reports, 1215 Jefferson Davis Highway, Suite 1204, Arlington, VA 22202-4302, and to the Office of Management and Budget, Paperwork Reduction Project (0704-0188), Washington, DC 20503.				
1. AGENCY USE ONLY (Leave blank)		2. REPORT DATE Feb. 14, 1994		3. REPORT TYPE AND DATES COVERED Final Report (7/1/91-2/28/94)
4. TITLE AND SUBTITLE An Integrated Approach to Seismic Event Location: II. Sources of Location Uncertainty for Teleseismic and Local Network Data			5. FUNDING NUMBERS PE61102F PR2309 TAG2 WUAZ F19628-91-K-0026	
6. AUTHOR(S) Cliff Frohlich				
7. PERFORMING ORGANIZATION NAME(S) AND ADDRESS(ES) Institute for Geophysics University of Texas at Austin 8701 North MoPac Expressway Austin, Texas 78759-8397			8. PERFORMING ORGANIZATION REPORT NUMBER	
9. SPONSORING/MONITORING AGENCY NAME(S) AND ADDRESS(ES) Phillips Laboratory 29 Randolph Road Hanscom AFB, MA 01731-3010 Contract Manager: Katharine Kadinsky-Cade/GPEH			10. SPONSORING/MONITORING AGENCY REPORT NUMBER PL-TR-94-2035	
11. SUPPLEMENTARY NOTES				
12a. DISTRIBUTION/AVAILABILITY STATEMENT Approved for public release; distribution unlimited			12b. DISTRIBUTION CODE	
13. ABSTRACT (Maximum 200 words) The locations of seismic events determined from travel times by independent agencies differ for at least three reasons, including differences in picking of or availability of the phases, effects produced by individual structural peculiarities of each station, and systematic mislocations caused by the choice of the travel time model used for relocation. The present study evaluates earthquake locations for events in three geographically diverse regions chosen to represent a broad spectrum of location problems. These are: Macquarie Ridge; Bucaramanga, Colombia; and Efate, Vanuatu. The evaluation methods include a comparison of locations reported by different agencies, an analysis of the sources of the variance of travel-time residuals, and a determination of the volume of groups of events thought to originate from a common source region. For the data analyzed it appears that station-dependent effects are a more significant source of location differences than are effects related to picking phase arrivals or choice of velocity model. Also, this study finds many situations where it seems inappropriate to utilize the strategy of minimizing travel time variance to improve location quality.				
14. SUBJECT TERMS Seismic event location, seismic strain, seismic discrimination			15. NUMBER OF PAGES 58	
			16. PRICE CODE	
17. SECURITY CLASSIFICATION OF REPORT Unclassified	18. SECURITY CLASSIFICATION OF THIS PAGE Unclassified	19. SECURITY CLASSIFICATION OF ABSTRACT Unclassified	20. LIMITATION OF ABSTRACT SAR	

Table of Contents

1. Introduction.....	1
2. Analysis of Individual Earthquake Groups	3
A. Macquarie Ridge.....	3
Background	3
Data Analysis	3
B. Bucaramanga, Colombia	8
Background	8
Data Analysis	15
C. Efate, Vanuatu	23
Background	23
Data Analysis	25
3. Evaluation of Sources of Location Uncertainty	30
A. Background	30
B. Misreading or Incorrect Identification of Phase Arrivals	32
C. Near-Station or Station-Path Effects	33
D. Velocity-Model Dependent Effects	34
E. Other Effects - Discussion.....	34
F. Summary and Conclusions.....	36
5. Results of Regional/Tectonic Interest.....	37
A. Macquarie Ridge.....	37
B. Bucaramanga, Colombia	38
C. Efate, Vanuatu	39
6. Acknowledgements.....	42
7. References	42

Accession For	
NTIS	CRA&I
DTIC	TAB
Unannounced	<input type="checkbox"/>
Justification	
By.....	
Distribution /	
Availability Codes	
Dist	Avail and / or Special
A-1	

1. INTRODUCTION

Typically, the report of an unusual seismic event in a remote area will generate a thorough investigation of previous historical seismic activity in that area. For historically reported activity, error analysis is complicated because phases for events occurring in different time periods are reported by different stations, arrivals are read by different individuals, and locations have been determined by different methods. For this reason it is useful to develop a framework for estimating location uncertainty that is not dependent on a formal statistical analysis such as proposed by Flinn (1965) or Boyd and Snoke (1984).

The most common methods for locating seismic events all use least squares to compare arrival time observations with times calculated using a regional or global earth model. In practice when different individuals or organizations independently locate seismic events they obtain slightly different results for three essential reasons:

- 1) Readings of the arrival times differ, due to unavoidable subjective differences in identifying, picking, and reading phase arrivals;
- 2) There exist systematic, station-dependent effects on seismic travel times of a magnitude which depends specifically on the details of the location method, which includes explicit or implicit decisions about the relative weights to be assigned to different arrivals or to different observing stations;
- 3) The appropriate velocity model for calculating travel times is always imperfectly known.

The present study will evaluate the relative contribution of each of these factors to location uncertainty by careful analysis of seismic locations in three quite different geographic regions (Table 1):

- 1) Macquarie Ridge - This remote region extends to about 1500 km south of New Zealand and possesses a high rate of shallow earthquake activity, but the only available phase data is from teleseismic stations;
- 2) Bucaramanga Nest, Colombia - This is an unusual intermediate-depth nest of earthquakes, observable both at regional and at teleseismic stations.
- 3) Efate Nest, Vanuatu - There exists a peculiar concentration of shallow earthquake activity just to the west of Efate Island, Vanuatu (formerly, the New Hebrides). To evaluate this activity we have observations from a regional seismic network and from temporarily deployed ocean bottom seismograph (OBS) stations.

Table 1. Comparative Characteristics of Three Hypocentral Groups

Geographic Region	Focal Depth	Data Type	Data Source
Macquarie Ridge	Shallow (~20 km)	Teleseismic	WWSSN Microfiche
Vanuatu	Shallow (~30 km)	Local	Field Observations
Bucaramanga	Intermediate (~160 km)	Teleseismic Regional	WWSSN Microfiche

Although both the character of the data and the nature of the location problem differs for each of these three data sets, in each case there are two basic types of data available for analysis:

- 1) Arrival time data - This includes arrival times read by the author and/or a close colleague which we can compare statistically with arrival times reported elsewhere;
- 2) Seismic event locations - These include locations determined by the author from specially selected groups of stations for comparison with other reported locations.

For all newly determined locations we use the TexFlex program developed specifically for this study and described in detail elsewhere (Frohlich, 1992; 1993). One objective of this study is to test the capability of the TexFlex program using a broad variety of input data. The TexFlex program is capable of locating seismic events using either user-supplied flat-earth velocity models, using teleseismic look-up tables like the Jeffreys-Bullen (1970) tables, or using the IASPEI91 teleseismic software described by Kennett (1991) and Kennett and Engdahl (1991). TexFlex can perform either single-event, joint hypocenter determination (JHD), or joint epicenter determination (JED) relocations. The program allows the user to choose a variety of phase weighting and station-grouping schemes. Individuals interested in obtaining the current version of the TexFlex software and an explanatory manual should contact the author by email.

The next section will summarize the arrival time data and locations for each of the three geographic regions. Then, the sections following will make some comparisons between location uncertainties for seismic events in the various regions, and draw some general conclusions about strategy for locating seismic events using travel-time-based methods. Finally, the last section will summarize some implications of the location analysis in each geographic region which may be important for individuals interested in the specific geographic areas studied.

2. ANALYSIS OF INDIVIDUAL EARTHQUAKE GROUPS

A. Macquarie Ridge

Background: The geographic region between New Zealand and about 60°S is renowned for its remoteness, its poor weather, and to seismologists (Ruff et al., 1989) for its abundance of large shallow earthquakes (Figure 1). Most of the seismic activity falls along a shallow bathymetric feature called the Macquarie Ridge which is the boundary between the Pacific and Australian plates.

The Macquarie Ridge is unusual seismically in that it possesses earthquakes having a broad variety of focal mechanisms, including strike slip, normal, and thrust mechanisms, as well as events with distinctly non-double-couple mechanisms (Frohlich et al., 1989). However, the vast majority of all earthquakes south of about 48°S have mechanisms with approximately horizontal P axes and approximately vertical B axes, consistent with predominantly strike-slip motion along the Macquarie Ridge (Figure 2)

There has been special interest in this region (e.g., Ruff, 1990) because on 23 May 1989 the largest ($M_w = 8.2$) submarine strike-slip earthquake in the world this century occurred there at about 52°S, 160°E. Recently Das (1993) used phase arrivals reported to the International Seismological Centre (ISC) and relocated earthquakes along the Macquarie Ridge using a JED method. Previously, the locations reported by the ISC (Figure 3) were the best available for seismic events in this area occurring since 1964. In the next section we shall explicitly compare the locations reported by the ISC and those reported by Das (1993) to locations determined explicitly for this study using a select group of stations.

Data Analysis: Because the Macquarie region is so remote from most of the world's seismic stations, only the largest earthquakes are recorded by most stations in the global network, and most earthquakes are located using only a few regional stations. For this reason we determine relocations using only a small group of stations, selected individually because they are as sensitive and reliable as any available stations, and selected as a group to represent the best possible azimuthal coverage for events in the Macquarie region.

The final station set chosen included 17 stations (Figure 4). This included two Canadian stations (FCC and MBC) at the appropriate distance to record PKP phases. However, because these station consistently had large residuals, and because phases observed there were often quite weak for Macquarie events, FCC and MBC were not used for the final relocations.

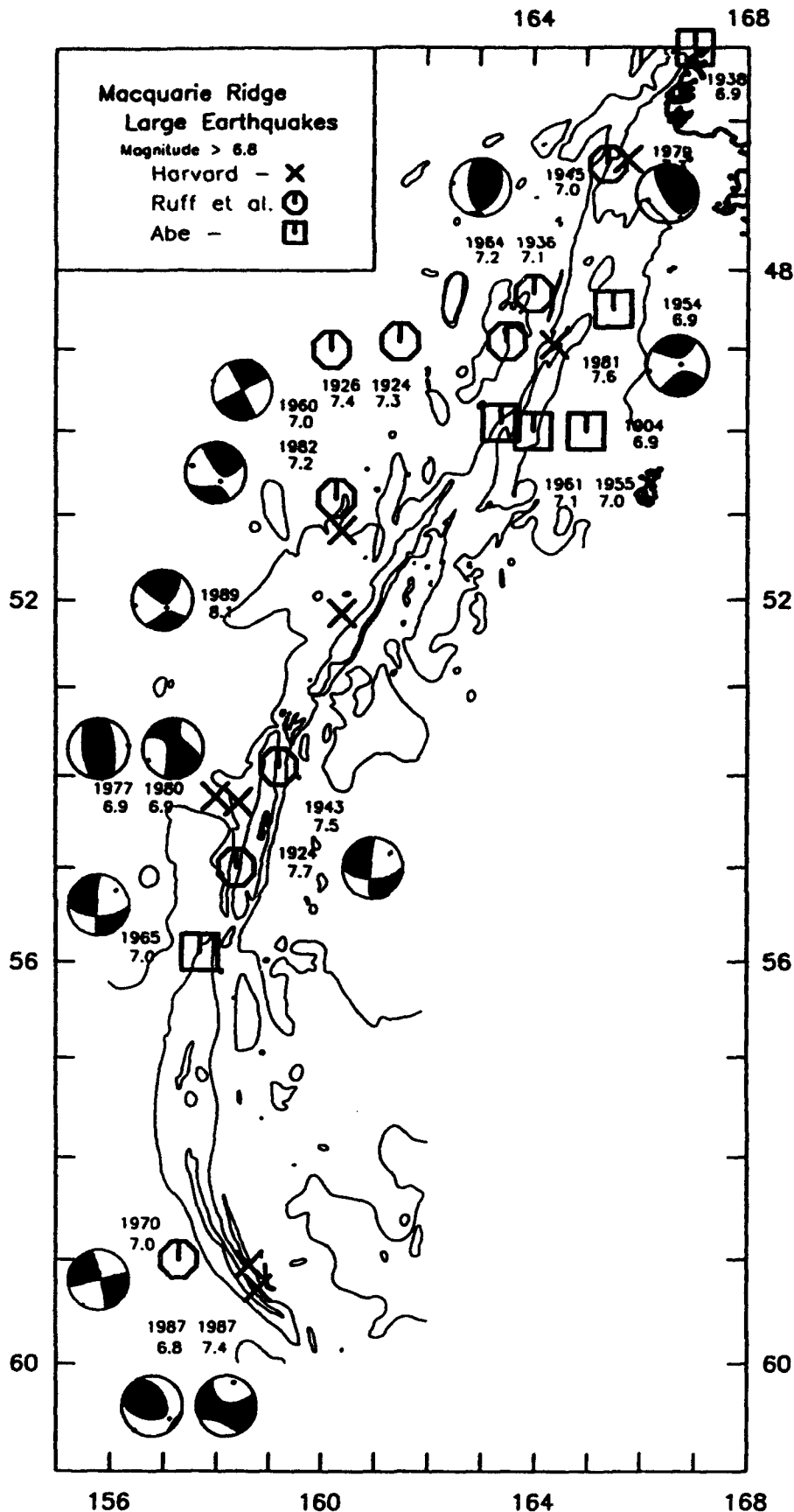


Figure 1. Map of locations of earthquakes with magnitudes exceeding 6.8 reported since 1904 along the Macquarie Ridge. For earthquakes occurring since 1977 locations and focal mechanisms are from the Harvard CMT catalog, and magnitudes are moment magnitudes M_w . Prior to 1977 locations and mechanisms are as reported by Ruff et al. (1989) if available. All remaining magnitudes are m_b from Abe (1981) and remaining locations are from Abe (1981).

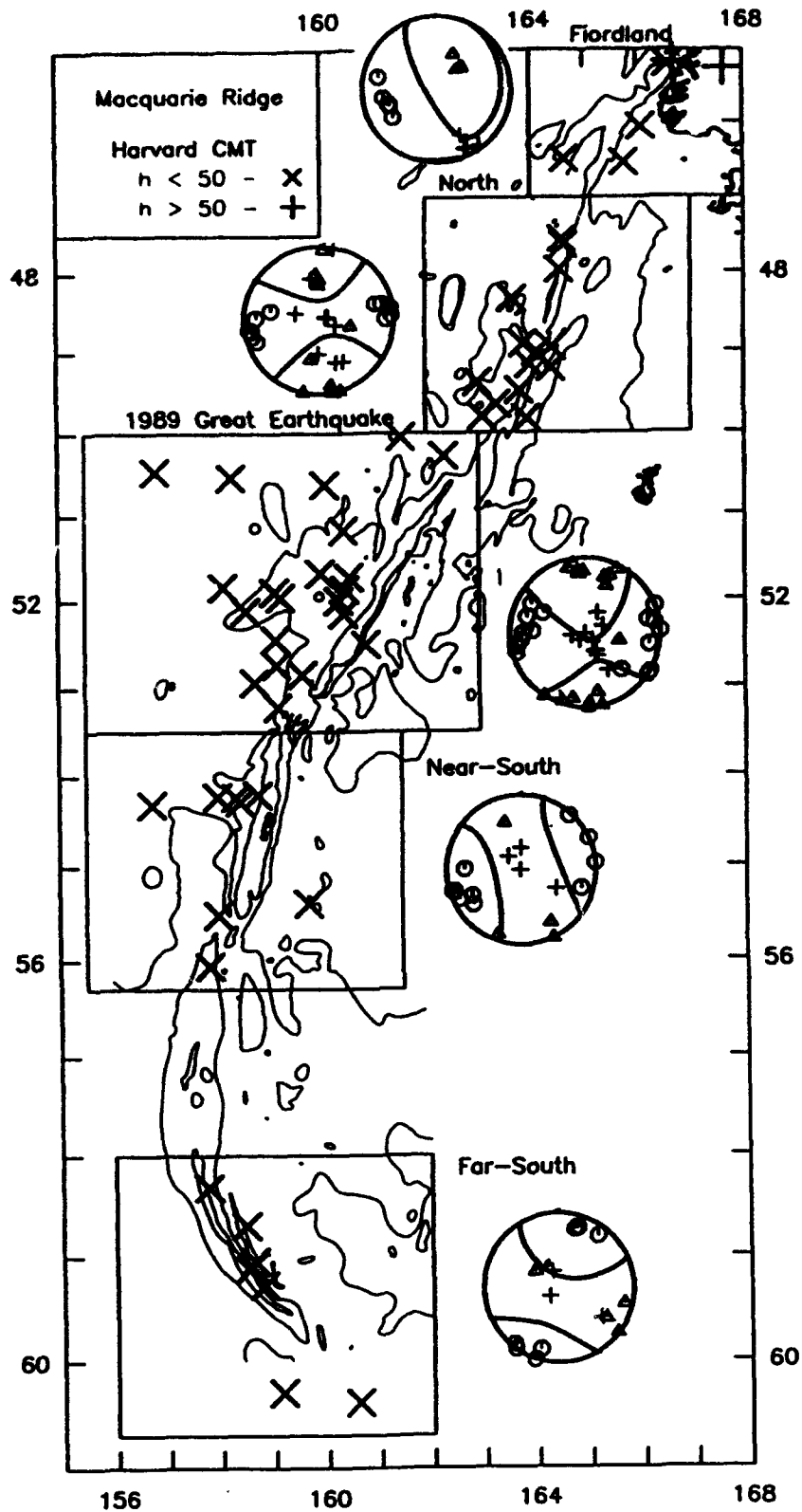


Figure 2. Map of locations of earthquakes with CMT reported by Harvard, and composite mechanisms for five geographic groups along the Macquarie Ridge. On focal spheres, triangles are T axes, octagons are P axes, and pluses are B axes for CMT of earthquakes in adjacent geographic region surrounded by box, while the plotted focal mechanism represents a composite mechanism determined by adding CMT for the individual earthquakes. For CMT with significant non-double-couple components (ratio of minimum to maximum principal moments exceeding 0.15), only the well-determined polar axis of the CMT is plotted. Except in the Fiordland subregion, note that the predominant mechanism type is strike-slip, with approximately horizontal P axis and approximately vertical B axis.

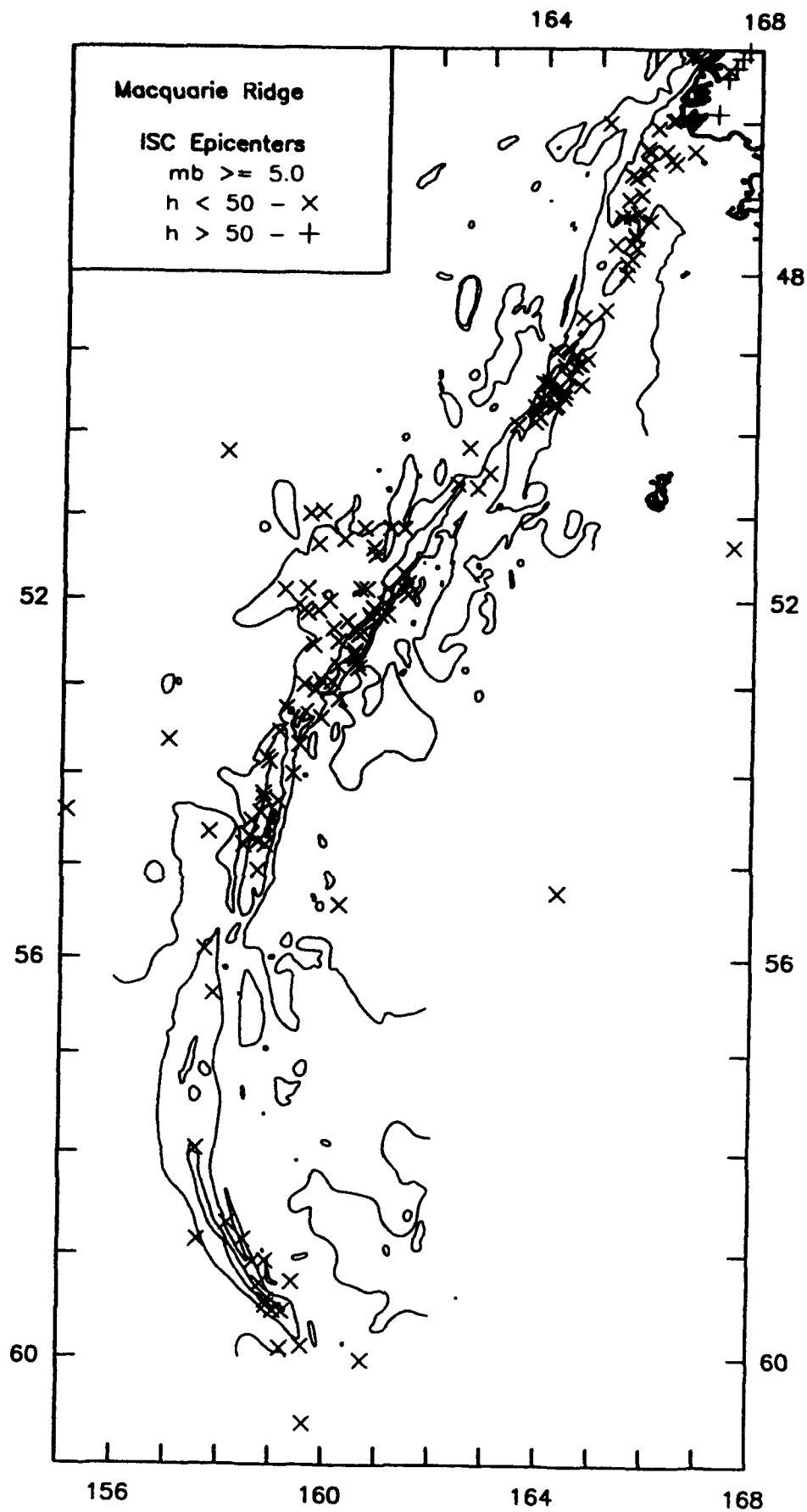


Figure 3. Map of earthquake locations reported by the ISC along the Macquarie Ridge for earthquakes occurring after 1964 and having body-wave magnitude m_b exceeding 5.0.

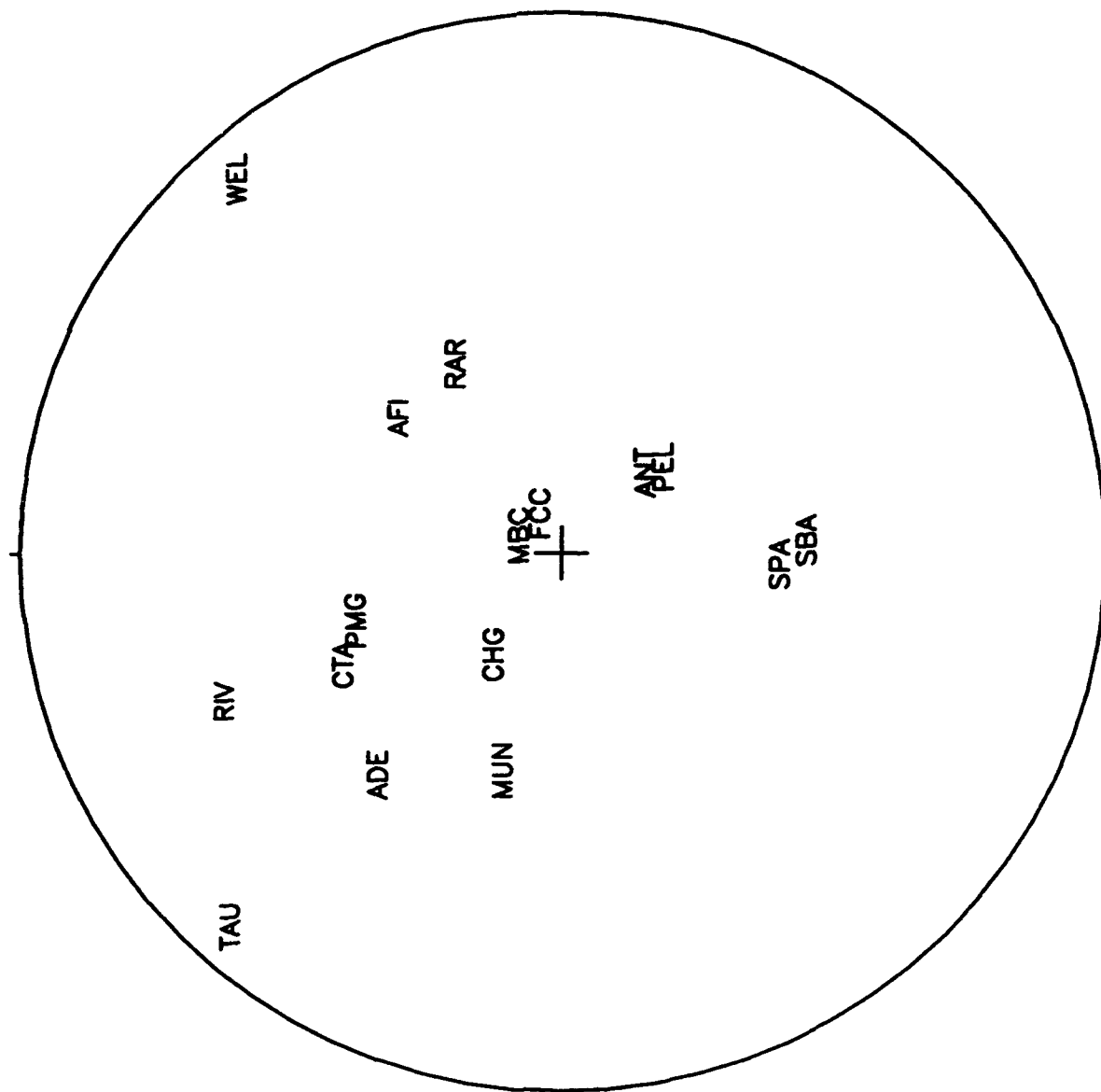


Figure 4. Focal sphere for hypothetical earthquake occurring at 52°S , 160°E showing the distribution of stations used in this study for relocations of Macquarie Ridge events. Stations near cross at center of plot correspond to rays leaving the focus vertically downward; stations at the edge correspond to rays leaving the focus horizontally. For these stations we personally reread all available P phases from WWSSN microfiche seismograms. The stations are: ADE - Adelaide, Australia; AFI - Afiamalu, Samoa; ANT - Antofagasta, Chile; CHG - Chiang Mai, Thailand; CTA - Charters Towers, Australia; FCC - Fort Churchill, Canada; LPB - La Paz, Bolivia; MBC - Mould Bay, Canada; MUN - Munding, Australia; PEL - Peldehue, Chile; PMG - Port Moresby, New Guinea; RAR - Rarotonga, Cook Islands; RIV - Riverview, Australia; SBA - Scott Base, Antarctica; SPA - South Pole, Antarctica; TAU - Tasmania University, Tasmania; WEL - Wellington, New Zealand.

Using the WWSSN microfilm collection at Columbia University, we obtained copies of P arrivals at these stations for as many earthquakes as possible. However, in practice it was only possible to find readable arrivals at the majority of stations for earthquakes with magnitudes exceeding m_b of 5.3 or so. Altogether we obtained phases for 53 earthquakes, including 36 with a sufficient data quality that we felt we could relocate them more accurately than did the ISC (Figure 5 and Table 2).

Of these 36 earthquakes, 1 were also relocated by Das (1993), who used the same phase arrival data as reported by the ISC, but obtained different locations because she determined station corrections using the JED method of Dewey (1971). A comparison of the locations reported by the ISC, by Das (1993) and this study (Figure 6) shows that median discrepancy between the locations of the ISC and this study was $D_{ISC-JHD} = 23$ km, while the median discrepancy between the ISC and Das (1993) locations was $D_{ISC-Das} = 12$ km. In a few cases, the difference in location was 80 km or more.

For the arrivals for 53 earthquakes reread especially for this study, 37% agreed with the ISC reported arrivals within 0.5 seconds (Table 3). However, 17% differed from the ISC reported arrival by 1.0 seconds or more. The mean difference between phase arrivals read by us and reported by the ISC was 0.37 seconds. Moreover, 15% of the phases we found and reread were not reported to the ISC. Also, there were ISC reported phase arrivals for 24% of the phases which we were unable to find after a careful search of the WWSSN microfiche seismograms.

Using the phases reread from the WWSSN seismograms, we relocated events in both the single-event and JED mode, and using both IASPEI91 and Jeffreys-Bullen (1970) travel time tables. For IASPEI91 travel times the use of JED reduced the variance of travel-time residuals (Table 4) from 1.25 sec^2 to 0.83 sec^2 , corresponding to a reduction in variance of 34%. For Jeffreys-Bullen travel times, the single-event variance was slightly larger (1.35 sec^2), but the variance for JED was somewhat smaller (0.71 sec^2), for a reduction of 48%.

B. Bucaramanga, Colombia

Background: About 160 km beneath Bucaramanga, Colombia (Figure 7), there exists a remarkable concentration of earthquake activity known as the Bucaramanga nest (Trygvasson and Lawson, 1970; Dewey, 1972). Since 1964 the ISC has reported an average of about 20 earthquakes/year with magnitude m_b of 4.7 or above occurring within the nest. Yet, careful studies using data from a temporary local network suggest that the active area has dimensions of only about 4-8 km and a total volume of about 11 km^3 (Pennington et al., 1979; Schneider et al., 1987; Frohlich and Kadinsky-Cade, 1993).

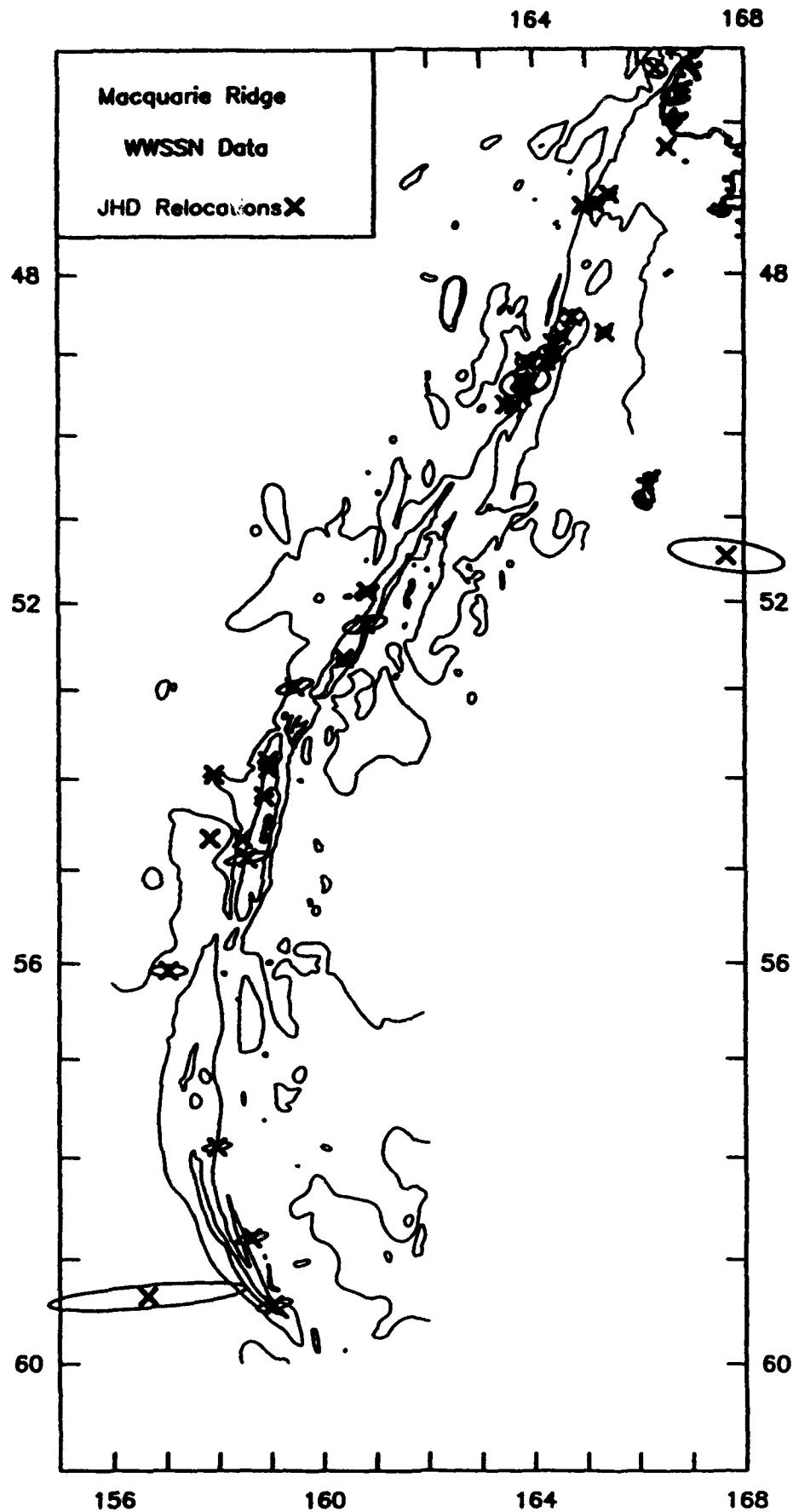


Figure 5. Map of earthquakes occurring along the Macquarie Ridge and relocated in this study using the JED method. Ellipsoids delineate the statistical uncertainty in the location, determined using the method of Willemann and Frohlich (1987).

Table 2. Epicenters near the Macquarie Ridge determined by using the JED method and arrival times read personally by the author.

Date	Hr Min Sec	Latitude °S	Longitude °E	Depth km	rms sec
11/ 8/66	2 43 56.01	49.109	163.905	20.00	1.20
4/ 5/66	11 57 41.83	54.872	158.610	20.00	1.32
4/28/66	1 15 38.44	49.148	164.161	20.00	1.04
5/25/66	13 20 57.00	52.677	160.362	20.00	0.37
6/28/67	14 34 5.54	47.004	165.408	20.00	0.87
9/20/67	9 39 15.36	49.676	163.653	20.00	0.74
9/20/67	10 30 55.59	49.641	163.514	20.00	0.60
9/23/67	7 2 7.00	49.555	163.834	20.00	0.40
5/ 8/68	11 0 7.76	57.882	158.004	20.00	0.56
9/25/68	7 2 51.56	46.363	166.553	20.00	0.56
6/11/70	16 46 37.87	59.367	156.511	20.00	1.26
3/23/72	23 10 0.74	45.266	166.400	20.00	0.65
4/ 1/72	23 51 24.31	49.347	163.778	20.00	0.50
4/ 2/72	0 17 45.37	49.378	163.876	20.00	2.10
12/24/72	20 30 58.81	52.259	160.765	20.00	1.52
6/ 7/73	2 43 31.83	53.890	158.956	20.00	0.43
10/19/73	0 13 1.68	54.701	158.371	20.00	0.66
4/ 6/74	12 16 24.72	48.814	164 470	20.00	0.83
6/ 5/74	11 44 22.12	54.719	157.258	20.00	0.23
9/10/75	15 48 54.96	49.413	163.824	20.00	0.32
9/16/75	0 0 50.26	47.094	165.242	20.00	0.83
1/ 7/76	6 59 12.32	47.119	164.899	20.00	0.89
7/21/77	11 53 22.21	53.821	158.921	20.00	0.82
7/21/77	12 34 32.95	53.919	158.117	20.00	0.42
5/24/78	6 12 2.48	52.972	159.560	20.00	0.83
8/28/78	8 4 14.06	48.842	165.209	20.00	0.80
5/25/81	5 25 14.61	48.580	164.767	20.00	1.29
5/30/81	9 47 19.52	49.009	164.488	20.00	0.40
5/23/84	5 16 37.86	51.881	160.883	20.00	0.80
8/ 2/65	13 19 55.73	56.099	156.888	20.00	1.28
9/12/64	22 7 3.74	48.923	164.341	20.00	0.42
9/03/87	6 40 14.05	58.803	158.607	20.00	0.49
9/03/87	8 1 36.46	59.452	159.027	20.00	0.55
2/07/80	10 59 13.70	54.194	158.943	20.00	0.46
4/02/72	0 39 2.10	49.407	163.905	20.00	0.53
6/26/71	22 2 24.30	51.510	167.593	20.00	1.63

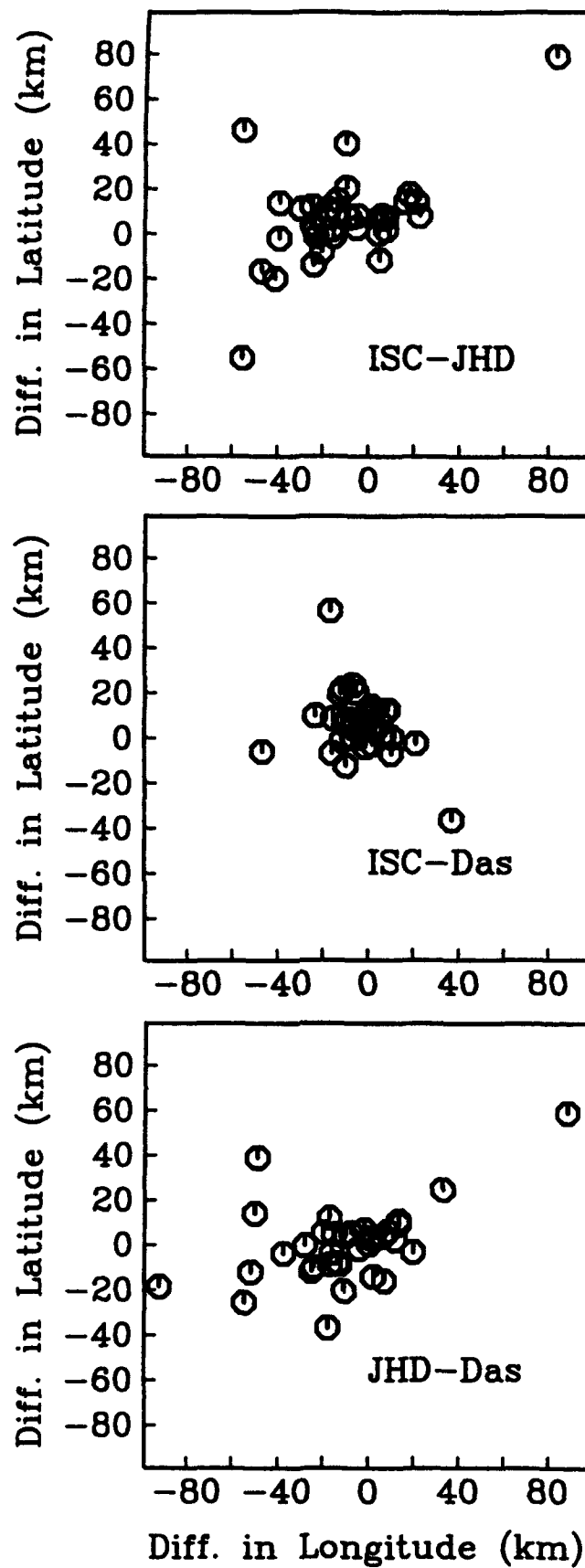


Figure 6. Differences in locations for 35 epicenters determined in this study (JHD), and those reported by the ISC and by Das (1993).

Table 3. Time differences between phase arrival picks reported by different sources. Results are presented as percentages of 585 picks at 16 stations for 53 earthquakes along the Macquarie Ridge, of 393 picks at 18 stations for 27 earthquakes near Bucaramanga, Colombia, and of 5,991 picks at 20 stations for earthquakes near Efate, Vanuatu. For Bucaramanga and Macquarie Ridge, sources of picks are arrivals reported by the ISC, and arrivals picked by the author and his colleagues. For Efate, the arrivals were picked independently by two different colleagues.

Time Difference (sec)	<i>Macquarie Ridge</i> Fraction of Total %	<i>Bucaramanga</i> Fraction of Total %	<i>Efate</i> Fraction of Total %
0.0 - 0.5	37	38	87
0.5 - 1.0	17	13	10
1.0 - 2.0	10	4	2
2.0 - 4.0	4	1	0
> 4.0	3	2	1
No ISC time reported	15	26	-
No phase found by author	24	16	-
Mean difference	0.37 [^] sec	0.39 [^] sec	0.21 [*] sec
Mean square difference	0.60 [^] sec ²	0.44 [^] sec ²	0.09 [*] sec ²

[^] - excluding differences larger than 4.0 sec

^{*} - excluding differences larger than 2.0 sec.

Table 4. Comparison of residual variance in seconds² for selected groups of earthquakes, for both single-event and JHD/JED relocations, and using different methods for calculating travel times. The residual variance is the square of the average RMS residual. All these locations utilized input data read personally by the author or his close colleagues.

Region	Single-Event IASPEI91	JHD/JED IASPEI91	Single-Event J-B	JHD/JED J-B
Macquarie Ridge (36 earthquakes)	1.25	0.83	1.35	0.71
Bucaramanga with pP and sP (26 earthquakes)	5.02	0.52	-	-
Bucaramanga with pP, no sP (26 earthquakes)	4.97	0.48	-	-
Bucaramanga - P only (26 earthquakes)	4.20	0.28	1.30	0.28

Region	Single-Event "best" model	JHD/JED "best" model	Single-Event layer over halfspace	JHD/JED layer over halfspace
Efate - P and S at all stations (21 earthquakes)	0.23	0.07	0.23	0.06
Efate - P and S except P only at land stations (21 earthquakes)	0.21	0.04	0.21	0.04

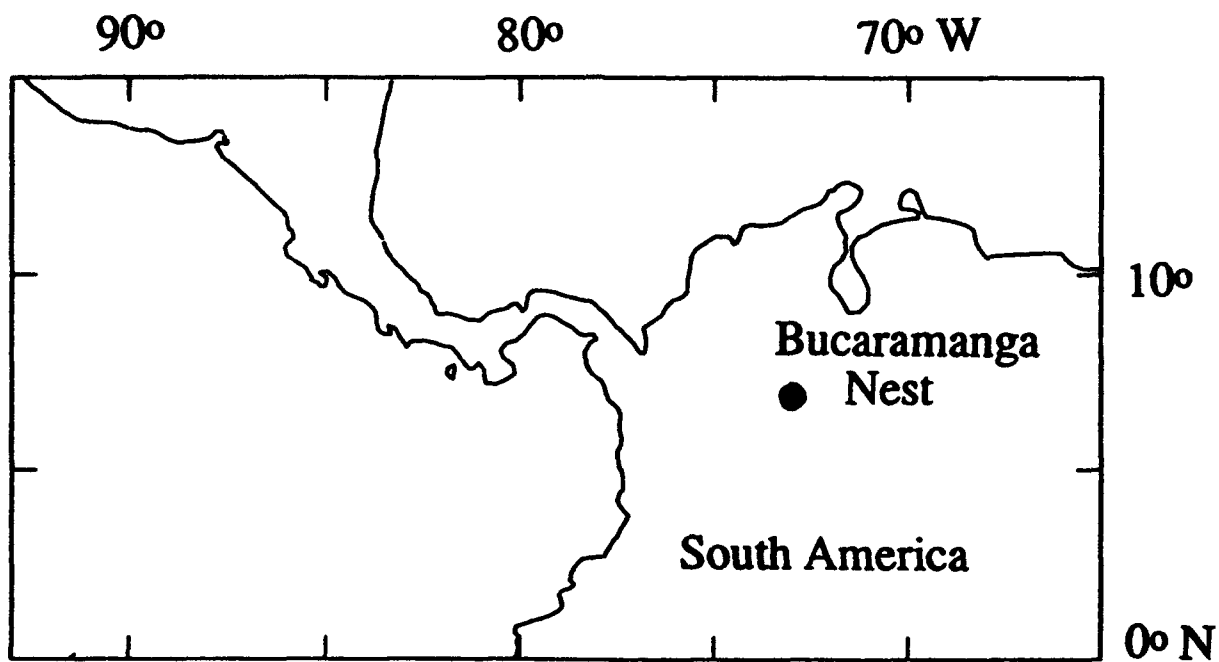


Figure 7. Location map for the earthquake nest near Bucaramanga, Colombia.

An important, fundamental, and presently unanswered question is what might cause such a persistent source of earthquake activity within the mantle. Presumably it is related somehow to the subduction of the Caribbean or Nazca plates beneath South America (Pennington, 1981). However, Schneider et al (1987) observed that P and T axes of focal mechanisms determined from the temporary local network were oriented almost randomly over the focal sphere (Figure 8). This is inconsistent with the usual models explaining intermediate focus earthquake mechanisms, where they are due to failure of a lithospheric plate due to bending, or to repeated motion along a particular weak failure surface.

Nevertheless, for several reasons the Bucaramanga nest provides a convenient source for testing and evaluating teleseismic location algorithms. Because the nest is so localized in space, for any particular data set or location method the nest volume or the variability in event locations is a measure of the relative accuracy of the location method (Frohlich and Kadinsky-Cade, 1993). Because the nest occurs well beneath the crust, teleseismic P phases are more likely to be clear and impulsive. Thus, the variability in the relative locations determined is attributable largely to systematic errors in the location method, rather than to intrinsic variability in the locations or to erroneous arrival time picks.

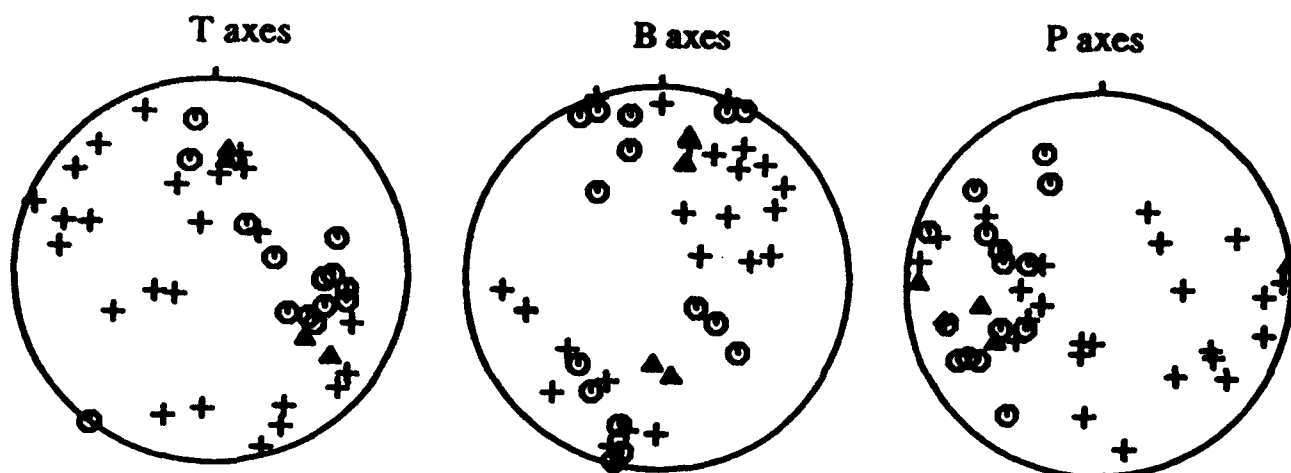
Data Analysis: Bucaramanga's location in northern South America allows us to obtain good station coverage in the northern, southern, and eastern azimuthal sectors. Using the WWSSN microfiche seismogram collection at Columbia University, we searched to find P arrivals at 21 stations (Figure 9) for 26 different earthquakes. Generally, we could pick P arrivals at the majority of these stations for earthquakes having body-wave magnitude m_b of 5.1 or greater.

The carefully determined phase arrivals and relocations of these 26 earthquakes provided the basic teleseismic data set for this study. For comparison we consider two other teleseismically determined set of locations; locations reported directly by the ISC, and relocations performed for this study using ISC-reported arrivals at a restricted set of stations (Table 5 and Figure 9). We also compare these locations to 27 hypocenters reported by Schneider et al (1987) determined using a temporary local network.

Because the nest is so localized in space, for map view and cross sectional comparisons we present pictures of the minimum-volume convex polyhedrons enclosing the hypocenters to display the relocations (Figure 10). Frohlich (1992) describes in detail an algorithm for determining the minimum-volume convex bounding polyhedron for a group of hypocenters. Essentially the polyhedron is formed by finding all the triangles determined by triples of hypocenters within the

T, B, and P axes for Bucaramanga focal mechanisms.

⊙ = Harvard CMT; ▲ = other teleseismic; + = Schneider et al. (1987)



"Sum" Focal Mechanisms

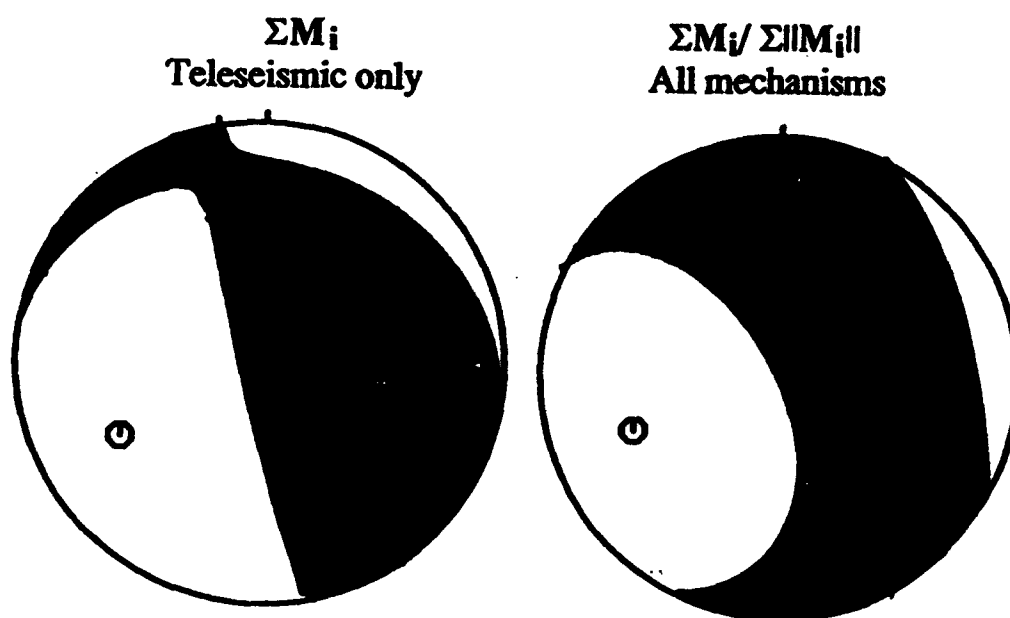


Figure 8. (Top) Summary of P, B and T axes of focal mechanisms for Bucaramanga earthquakes. Symbols are: octagons - Harvard CMT; triangles - other teleseismically determined mechanisms reported by Pennington (1981); pluses - mechanisms determined from temporary local network data by Schneider et al. (1987).

(Bottom) Composite focal mechanism determined by adding together moment tensors for (bottom left) Harvard CMT and other teleseismic earthquakes; and (bottom right), all available mechanisms, each normalized by dividing by the scalar seismic moment.

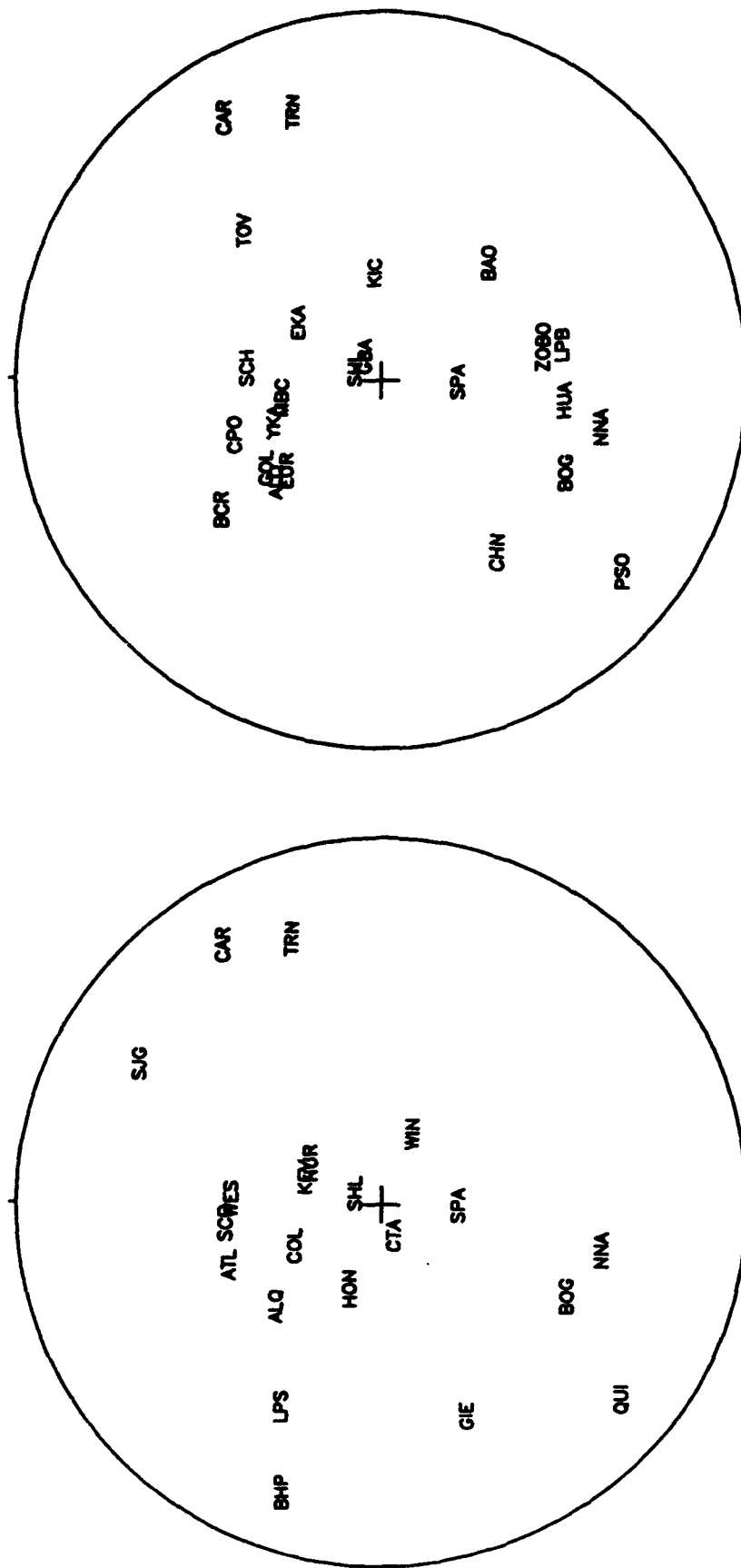


Figure 9. Focal sphere for hypothetical earthquake occurring at 6.8°N, 73°W showing the distribution of stations used in this study for relocations of Bucaramanga events. (Left) For these 21 stations we personally reread all available P, pP, sP, or PkP phases from WWSSN microfiche seismograms. The stations are: ALQ - Albuquerque, New Mexico; ATL - Atlanta, Georgia; BHP - Balboa Heights, Panama; BOG - Bogota, Colombia; CAR - Caracas, Venezuela; COL - College, Alaska; CTA - Charters Towers, Australia; GIE - Galapagos Island; KEV - Kevo, Finland; HON - Honolulu, Hawaii; LPS - La Palma, El Salvador; NNA - Nana, Peru; NUR - Nurmijarvi, Finland; QUI - Quito, Ecuador; SCP - State College, Pennsylvania; SJG - San Juan, Puerto Rico; SHL - Shillong, India; SPA - South Pole, Antarctica; TRN - Trinidad; WES - Weston, Massachusetts; WIN - Windhoek, Namibia. (Right) For these 28 stations we used P arrival times reported by the ISC: ALQ; BOG; CAR; NNA; SHL; SPA; TRN; BAO - ; Brasilia Array, Brazil; BCR - Bucaramanga, Colombia; BMO - Blue Mountains Array, Oregon; CHN - Chinchina, Colombia; CPO - Cumberland Plateau, Tennessee; EKA - Eskdalemuir, Scotland; EUR - Eureka, Nevada; GBA - Gauribidanur, India; GOL - Golden, Colorado; HUA - Huancayo, Peru; KIC - Kusan Boca, Ivory Coast; KOD - Kodaikanal, India; LPB - La Paz, Bolivia; MBC - Mould Bay, Canada; PNS - Penas, Bolivia; PSO - Pasto, Colombia; SCH - Shefferville, Canada; UBO - Uinta Basin Array, Utah; TOV - El Tocuyo, Venezuela; YKA - Yellowknife Array, Canada; ZOBO - Zongo, Bolivia.

Table 5. Hypocenters in the Bucaramanga nest relocated using the JHD method and P PKP, and pP times arrival times read personally by the author.

Date	Hr Min Sec	Latitude °N	Longitude °W	Depth km	rms sec
2/26/65	23:36:14.27	6.796	72.921	158.53	0.79
7/30/65	7:20:10.15	6.819	72.935	159.24	0.49
9/11/66	17:38: 4.80	6.831	72.910	157.47	0.71
3/21/67	18:11:44.43	6.776	72.925	159.91	0.65
7/29/67	10:24:26.22	6.832	72.995	166.56	0.78
5/ 7/68	9: 0:29.98	6.850	72.960	162.17	0.68
8/18/72	20:58:19.17	6.802	72.997	161.59	0.74
4/23/73	16:26:10.71	6.785	72.993	160.73	0.89
7/ 8/73	4: 3:36.52	6.802	72.926	160.70	0.62
9/ 5/74	7:47:43.13	6.840	73.005	168.33	0.83
3/13/76	21:44:42.41	6.806	72.906	161.06	0.56
4/ 1/76	19:21:16.39	6.839	73.009	158.06	0.65
3/23/77	2:11:15.65	6.801	72.889	161.38	0.42
7/ 2/78	2:49:19.18	6.743	72.938	164.40	0.61
1/14/79	19:20:31.45	6.742	72.983	161.70	0.88
3/11/79	12:16:20.29	6.805	72.956	161.28	0.70
8/15/80	21:30:47.34	6.749	72.984	160.42	1.05
12/13/81	21:40:37.68	6.788	72.956	157.49	0.58
5/19/83	23:22:16.16	6.825	72.934	161.05	0.47
8/29/83	8:24:25.33	6.806	72.976	156.77	0.74
11/ 4/84	13:14:21.32	6.804	72.980	161.60	0.44
6/26/85	23:44:55.48	6.799	72.921	159.74	0.84
12/ 3/85	17:52:25.09	6.777	72.911	159.85	0.32
3/31/86	1:19:25.23	6.846	72.976	156.06	0.85
6/29/86	20:11:52.29	6.859	72.949	165.05	0.66
10/31/86	7: 5:54.05	6.826	73.001	159.94	0.35

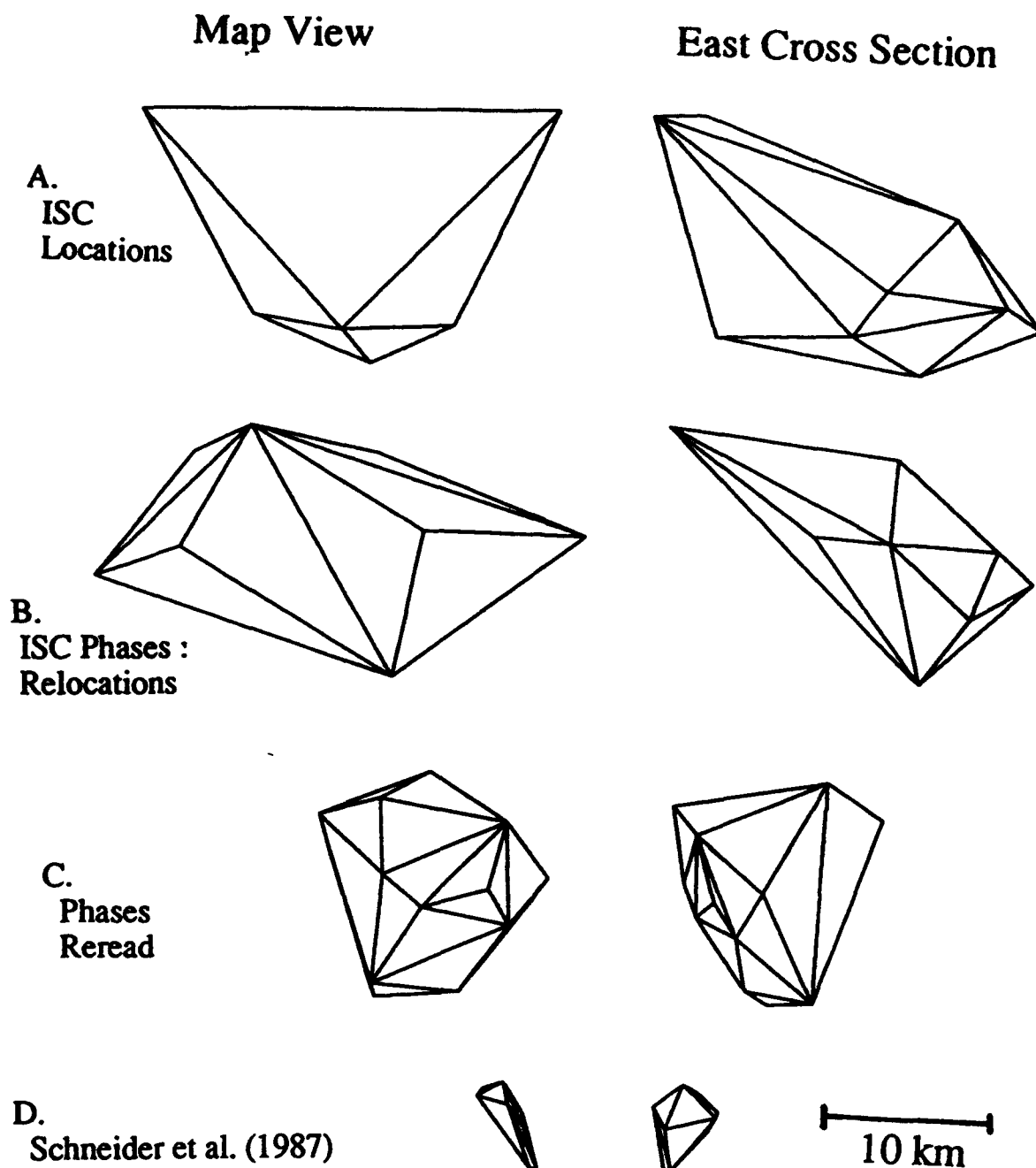


Figure 10. Bounding polyhedrons for four sets of hypocentral locations in the Bucaramanga nest. At left are map views of the upper surfaces of polyhedrons; at right are cross sectional views of the front side of the polyhedrons as viewed from the east. The four sets of locations are: A) Locations as reported by the ISC for 26 hypocenters occurring between 1965 and 1986; B) Relocations of the same 26 hypocenters determined for this study with a weighted least-squares JHD method using phase arrivals reported by the ISC at 28 selected stations; C) Relocations for the same 26 hypocenters, relocated with a weighted least-squares JHD method using P, PKP, and pP data personally reread by the author at 18 selected stations; D) Locations for 27 hypocenters reported by Schneider et al. (1987), determined from a temporary local network.

group, then, the minimum volume convex polyhedron is just the region in space enclosed by these triangles.

It is possible to compare the absolute locations for the 26 earthquakes which possessed three different locations, i.e., locations reported by the ISC, relocations determined for this study using phase arrivals reported by the ISC, and relocations determined for this study using phase arrivals read by the author. These comparisons (Figure 11) indicate that the median discrepancy between events in the first and second sets of locations (reported and relocated ISC) was $D_{12} = 17.3$ km, while the median discrepancy between the first and third sets (reported ISC and this study) was $D_{13} = 12.4$ km.

For the 393 earthquake arrivals reread especially for this study, 38% agreed with the ISC reported arrivals within 0.5 sec (Table 3). However, 7% differed from the ISC reported arrivals by 1.0 seconds or more. The mean difference between phase arrivals read by us and reported by the ISC was 0.39 seconds. Moreover, 26% of the phases we found and reread were not reported to the ISC. Also, there were ISC-reported phase arrivals for 16% of the phases which we were unable to find after a careful search of the WWSSN microfiche seismograms.

Using the phases reread specifically for this study, we performed relocations of the 26 earthquakes using both IASPEI91 and Jeffreys-Bullen (J-B) travel times, and using both single-event and JHD location algorithms (Table 5). Although the variance of travel time residuals (Table 4) obtained using IASPEI91 times were somewhat larger than those obtained using J-B times, this was mostly because we did not have J-B tables for depth phases such as pP and sP. Thus these phases did not constrain the relocations, and while the resulting variances were small the best so obtained was far less localized than that obtained with the IASPEI91 tables (Table 6).

The volume of the bounding polyhedron depended strongly on exact phases, travel time model, and method of location used (Table 5). Bounding polyhedrons for single-event relocations had volumes of 30-200 times larger than JHD relocations. This was caused by the occurrence of systematically large residuals averaging 4-6 seconds at two stations, BHP and SJG, which also produced variances for 4-5 sec^2 for all single-event IASPEI91 relocations (Table 4). Thus, for the IASPEI91 relocations using JHD reduced the variance by 90% or more, to about 0.50 sec^2 and less. The effect of using different methods to calculate travel times was less pronounced. For example, for the JHD relocations the bounding polyhedron volume was 2,135 km^3 for the J-B relocations, and 687 km^3 for the IASPEI91 relocations utilizing P, PKP and pP phases.

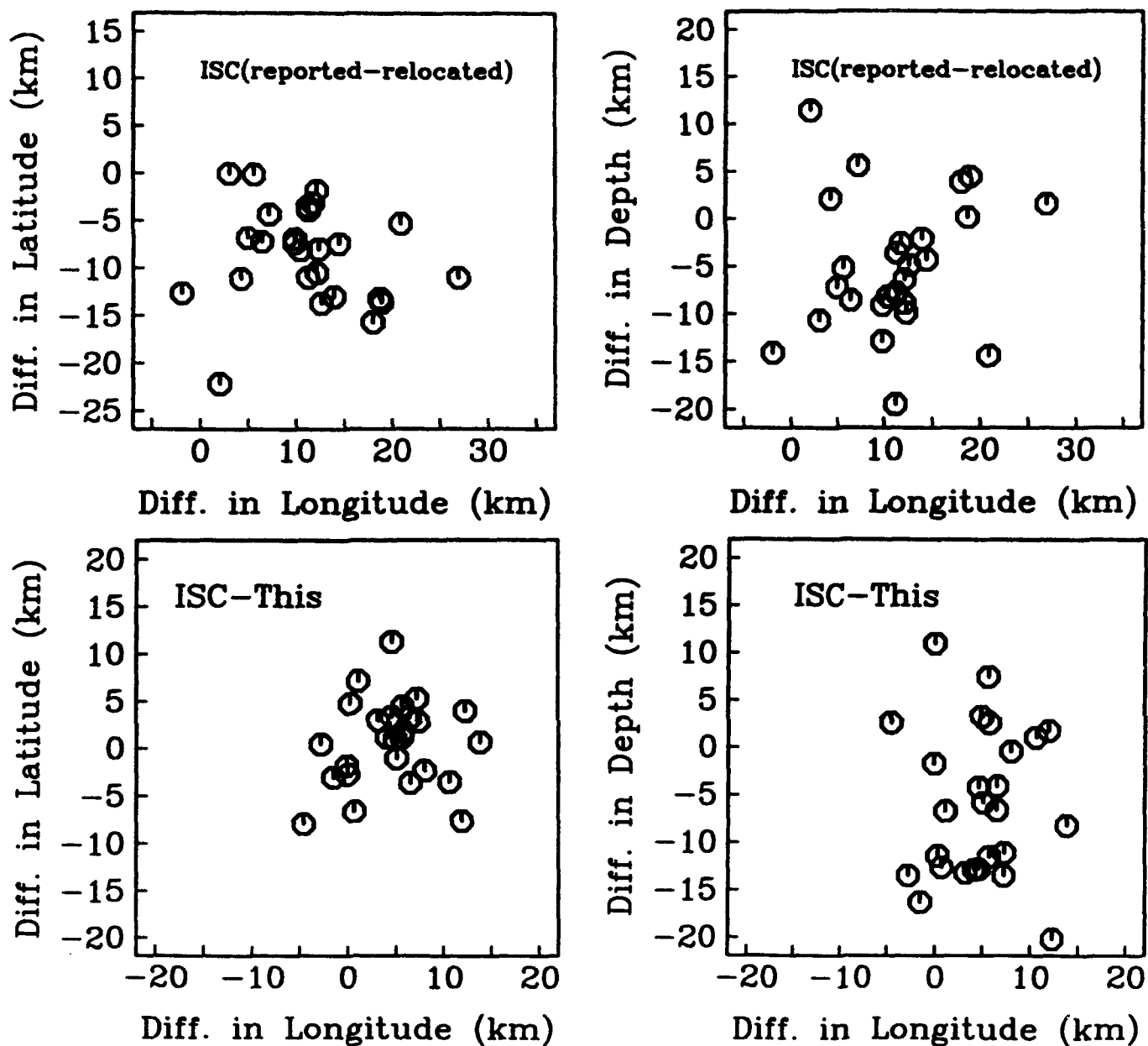


Figure 11. Differences in locations for 26 epicenters located by three different methods: 1) locations reported by the ISC; 2) locations relocated using phases reported to the ISC; and 3) locations determined using phases reread for this study. Top panels summarize differences between the first two sets of locations, and the bottom two panels summarize differences between the first and third sets.

Table 6. Comparison of volume of smallest convex polyhedron enclosing relocated groups of 26 earthquakes in Bucaramanga, Colombia, and 21 earthquakes in Efate, Vanuatu, for both single-event and JHD/JED relocations, and using different travel time tables. All these locations utilized input data read personally by the author or his close colleagues.

Travel time, phase data	Single-Event	JHD
<i>Bucaramanga, Colombia</i>		
IASPEI91, P, PKP, pP and sP	33,941 km ³	1,176 km ³
IASPEI91, P, PKP and pP	45,766 km ³	687 km ³
IASPEI91, P and PKP only	208,025 km ³	851 km ³
J-B, P only	17,819 km ³	2,135 km ³
<i>Efate, Vanuatu</i>		
"best" model, P and S at all stations	5,502 km ³	4,321 km ³
layer over halfspace, P and S at all stations	7,227 km ³	5,022 km ³
"best" model, P and S except P only at land stations	8,553 km ³	6,726 km ³
layer over halfspace, P and S except P only at land stations	7,202 km ³	7,246 km ³

C. Efate, Vanuatu

Background: Vanuatu (formerly, the New Hebrides) is a nearly linear island chain (Figure 12) situated at the convergent boundary between the Indo-Australian and Pacific plates (Pascal et al., 1978). Near the island of Efate the convergence rate is about 11 cm/yr and the direction is approximately normal to the New Hebrides trench (Prevot et al., 1991). About 200 km to the north there is a peculiar region of shallow bathymetry known as the d'Entrecasteaux Ridge (DR) which clearly affects the regional tectonics (Collot and Fisher, 1991; Fisher et al., 1991). The collision of the DR with the New Hebrides trench appears to cause Quaternary uplift and tilting on the islands of Santo and Malekula (Taylor et al., 1980; 1987) and reactivation of normal faults on the islands of Santo, Maewo and Pentecost (Isacks et al., 1981). Moreover, while the New Hebrides trench is clearly evident west of Efate and the islands to the south, it disappears between Efate and Malekula, and the western parts of the islands of Malekula and Santo lie along the extension of the New Hebrides Trench.

The DR may influence the ongoing seismicity of the central Vanuatu region as well. Just west of Efate near 17.5°S, 168.0°E there is a highly active zone of shallow seismic activity known as the Efate nest (Figure 12). The origin of the Efate nest is uncertain. Chatelain et al. (1986) suggested this area forms a seismic boundary between a quiescent asperity to the north and a seismically active segment in the south. Prevot et al. (1991) observed slow seismic velocities for seismic waves traversing the Efate nest region. They suggest that the Efate nest may occur where a previously subducted remnant of the DR trails to the south of its bathymetric expression and interacts with the overlying plate.

The most significant uncertainty in the interpretations of Chatelain et al. (1986) and Prevot et al. (1991) concerns the focal depth of the earthquakes in the Efate nest. All their data comes from a regional seismograph network operated between 1978 and 1989 at up to 23 sites on various islands of Vanuatu by the Institut Français de Recherche Scientifique pour le Développement en Coopération (ORSTOM). Because of the geometry of the islands forming Vanuatu fix the geometry of the ORSTOM land network, it is difficult to obtain reliable depths for earthquakes occurring northwest of Efate and south of Malekula.

In order to more accurately determine earthquake focal depths, between June and August of 1989 ORSTOM and the University of Texas at Austin deployed ocean bottom seismographs (OBS) at 26 sites within this region. While the data collected by the OBS/land network was not originally collected or analyzed for the present study, it provides a unique data set for comparison with the

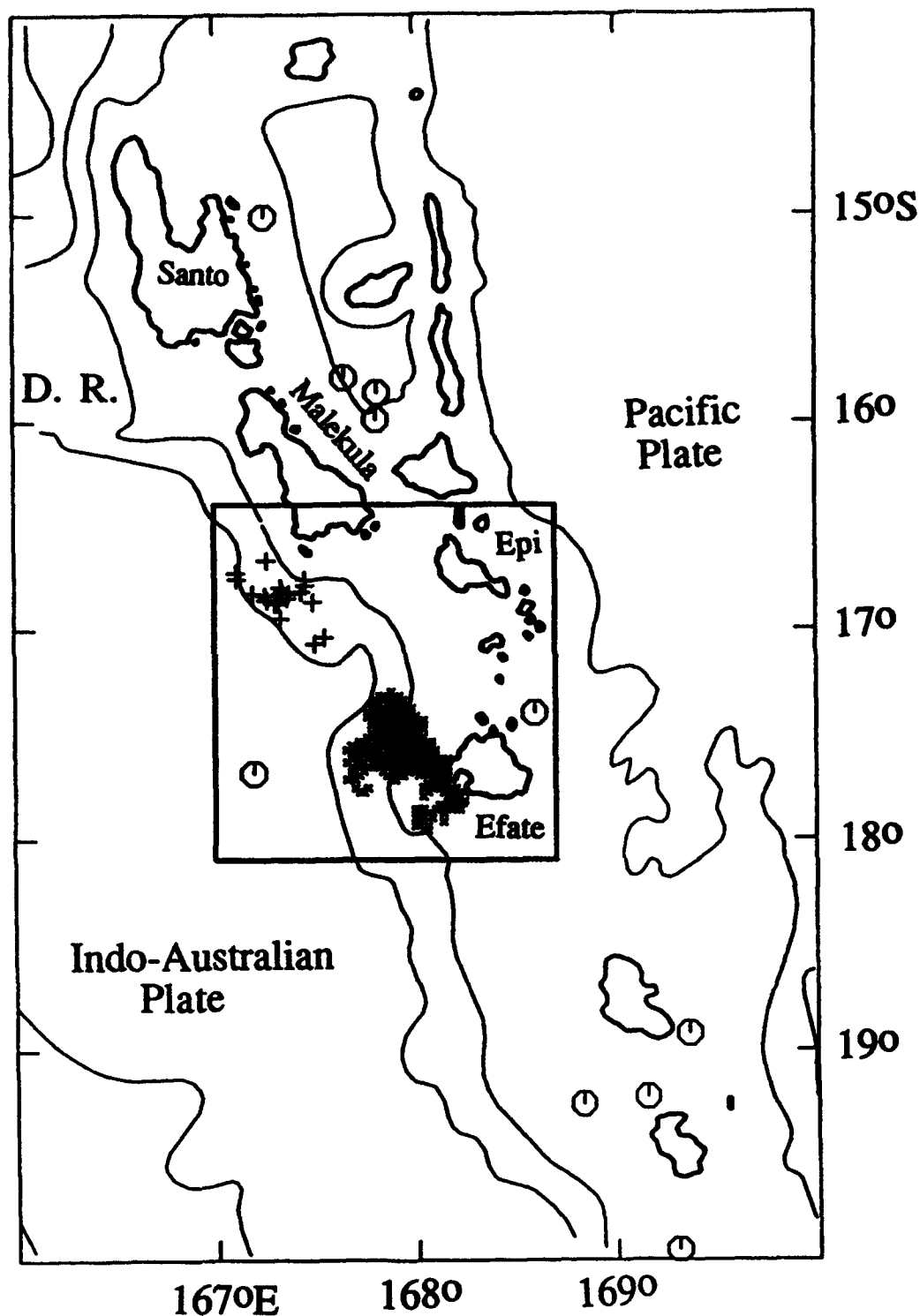


Figure 10. Map the central New Hebrides island arc, with major islands of Vanuatu labeled. Box delineates region of map in Figure 13 describing 1989 OBS/island network. Contours are in meters. D'Entrecasteaux Ridge (labeled "DR") lies north of westward bend in 4000 m contour occurring west of Santo and Malekula. Plus symbols ("+") are locations reported by Roecker et al. (1988) in region with unusual deep focal depths. Circles are locations reported by ISC for earthquakes with arrivals reported by OBS array in Table 8. Shaded area west of Efate delineates the Efate nest— a region of intense shallow earthquake activity studied by Chatelain et al. (1986); within the shaded area between 1977 and 1988 the ORSTOM land network reported 30 or more earthquakes occurring within each $.02^\circ \times .02^\circ$ square, with each location constrained by at least 7 P arrivals and 4 S arrivals.

two teleseismic data sets. It also provides a reasonable test of the application of the TexFlex location program as applied to local network data.

Data Analysis: The field experiment consisted of two deployments of 13 digital OBS instruments each (Figure 13) between 22 June and 19 August, 1989, for a total deployment time of 42 days. The OBS stations in this study operated in a triggered mode as described by Frohlich et al. (1990), with the trigger depending on the ratio of absolute signal amplitudes determined over a short-term (1.6 second) and a long-term (411 second) interval. A continuously operating circular memory buffer held 6-10 seconds of data, so that when the OBS triggered a tape drive recorded the signal in the buffer as well as the signal following the trigger. All OBS had a vertical-component 4.5 Hz seismometer. In addition, all but two instruments had two 4.5 Hz horizontal-component seismometers. One remaining instrument had a hydrophone and one 4.5 Hz horizontal-component seismometer (OB5 and O21); the last instrument had a 2.0 Hz vertical-component seismometer and a 10 Hz horizontal component seismometer (OB8 and O26). The sampling interval for recording was 25.056 ms, with data low pass filtered with a cut-off frequency of 15 Hz prior to recording.

The data also included records from nine land stations in the ORSTOM regional network (Figure 13). These stations all have vertical component, 4.5P Hz seismometers. Data are telemetered to a base station where, if enough stations trigger, data are recorded on magnetic tape and by a multichannel oscillograph system. Experience suggests that the system records all earthquakes in the study area with magnitudes M_L larger than about 2.7 (Chatelain et al., 1986).

Altogether the land and OBS networks recorded about 40,000 blocks of data during this experiment. For the initial data processing we examined each block individually to identify seismic signals. For the events identified as earthquakes occurring within the Efate nest (Figure 14), two different seismologists independently picked the times of P and S phases, and evaluated the quality of the arrival time picks by grading them from 1 to 4, corresponding approximately to uncertainties of <0.1 sec, <0.3 sec, <1.0 sec, and >1.0 sec, respectively. For 5,991 arrivals assigned pick qualities 1 and 2, the mean difference in picked times was 0.21 sec (Table 3), and 90% of all differences were less than 0.55 seconds.

Of 3443 seismic events recorded during the field study, 28 were airgun shots that we fired during the field program, 18 were regional or teleseismic earthquakes reported by the International Seismological Centre (Figure 12), and 74 were observed only at stations in the land network without triggering any OBS. We further classified 2563 of these events as unlocatable because they possessed P phases of pick quality 3 or better at 2 or fewer stations, or at 3 stations with no S

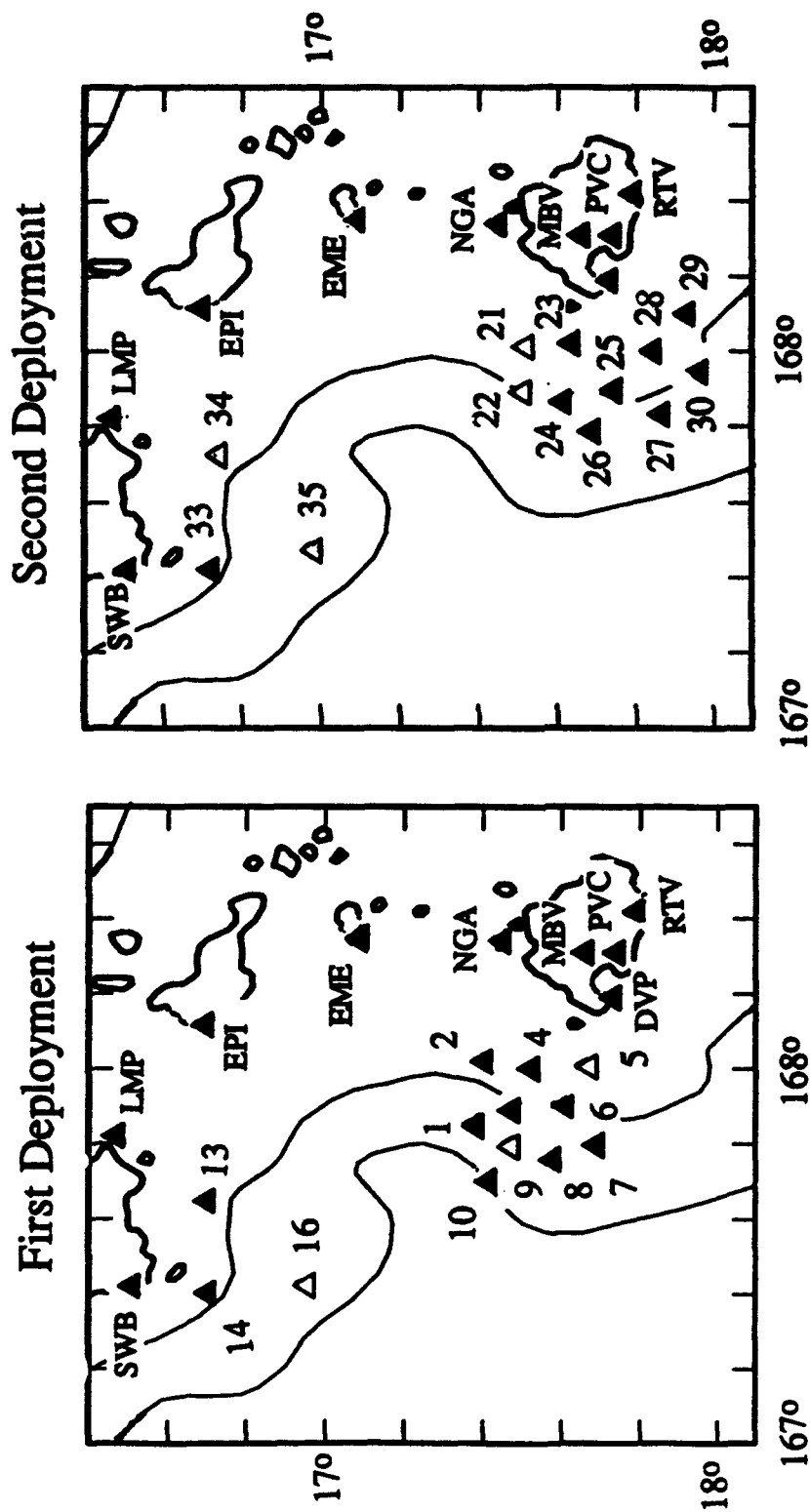


Figure 13. Location of island and OBS stations for the two OBS deployments. Map at left shows station locations for first deployment (22 June - 16 July); map at right is for second deployment (21 July - 19 August). Filled triangles are stations recording ten or more earthquakes; open triangles recorded fewer than ten. Contours are at 2000 m and 4000 m.

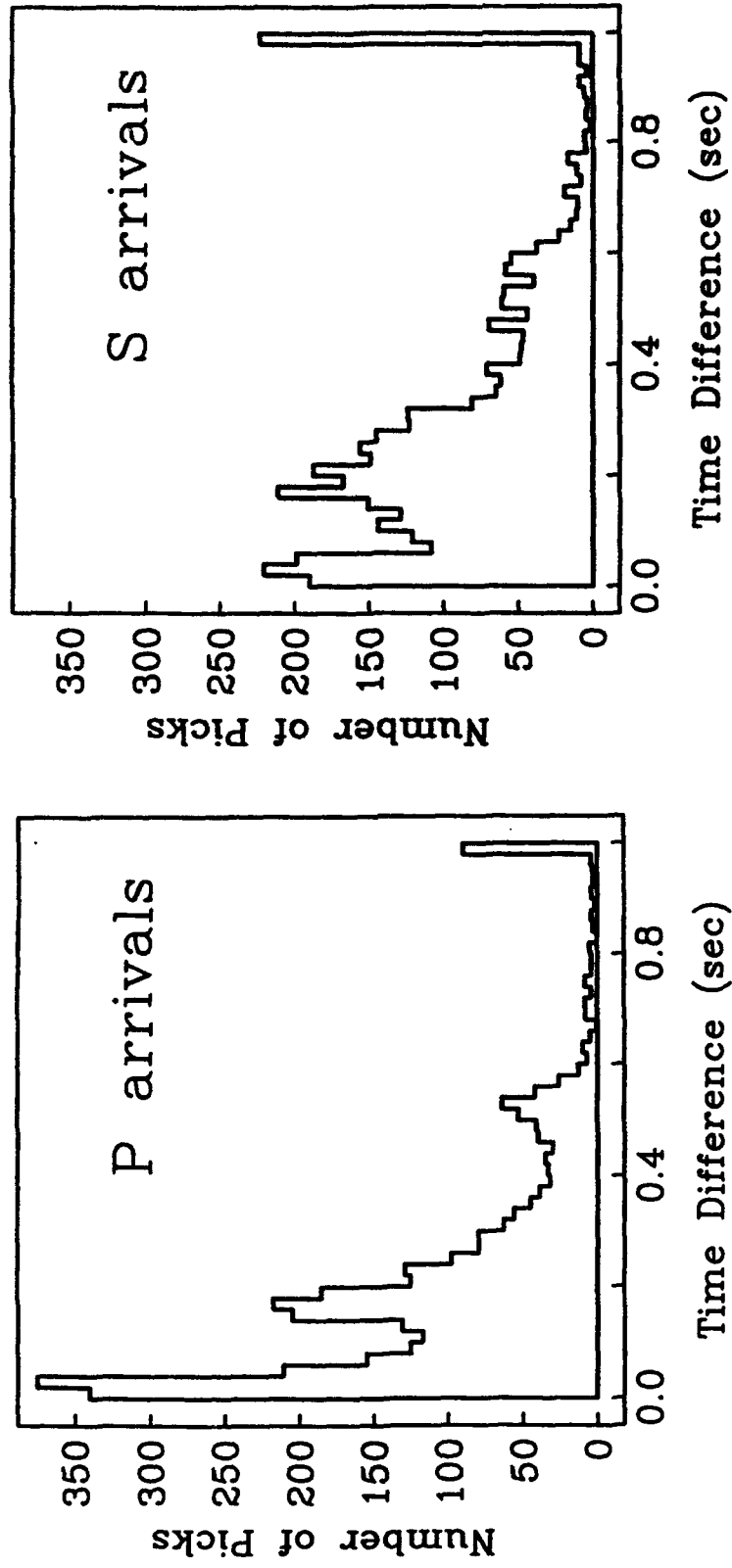


Figure 14. Histogram of difference in P and S phase arrival times as picked independently by two individuals.

phases of pick quality 3 or better. Unfortunately, none of the earthquakes reported by the ISC were well-recorded enough by the OBS network to locate independently.

For the remaining 760 earthquakes, we obtained preliminary locations using TexFlex in the single event model (Figure 15). Our "best" velocity model was similar to those determined by Prevot et al. (1991) for the region beneath and just west of Efate. For arrivals at the OBS stations, the "best" model had three layers of thickness 10 km overlying a halfspace, with velocities of 5.0 km/sec, 7.1 km/sec, 7.3 km/sec, and 8.0 km/sec. At the land stations, the layer thicknesses were 10 km, 20 km, and 10 km, and the velocities were 5.2 km/sec, 6.8 km/sec, 7.6 km/sec, and 8.0 km/sec. For comparison, we also performed all relocations assuming a simpler model consisting of a layer of velocity 5.5 km/sec overlying a halfspace with velocity 8.0 km/sec. For both the "best" and the "layer over a halfspace" models we assumed that V_P/V_S was 1.78. The remainder of our analysis concerns evaluation of the subset of these 760 earthquakes which occurred within the Efate nest.

To obtain precise relative locations for events within and near the Efate nest we first applied the JHD method to an especially well-recorded subset of 21 earthquakes in order to determine station corrections. At least four OBS stations and two land stations recorded each of these earthquakes, with an azimuthal gap of 230° or less. Some experimentation revealed that the JHD station corrections depended strongly on the particular combinations of land stations data used.

We finally chose to relocate using both P and S data from OBS stations while using P arrival data only from the land stations DVP, RTV, MBV, and NGA. With this scheme the (S - P) times at three-component OBS stations constrained focal depths of events, while P times at the more distant vertical-component land stations influenced the lateral position of the events. The resulting station corrections were positive at the land stations in the east (NGA, MBV and RTV), quite negative at four stations near the center of the network (OB3, OB4, OB7 and O25), and quite positive for two of the OBS stations at the western edge of the network (O10 and O27). Applying these station corrections reduced the variance for the 21 especially well-recorded earthquakes from 0.21 sec^2 to 0.04 sec^2 (Table 4).

While the application of station corrections did reduce the variance of travel time residuals, it had only a minor effect on the localization of the group of 21 events, as measured by the volume of the bounding polyhedron (Table 6). Also, there was no systematic difference between using the "best" velocity model and the layer-over-halfspace model.

Finally, to evaluate the overall spatial geometry of the events recorded from within the Efate nest, we applied the station corrections obtained above to relocate a larger set of 92 earthquakes

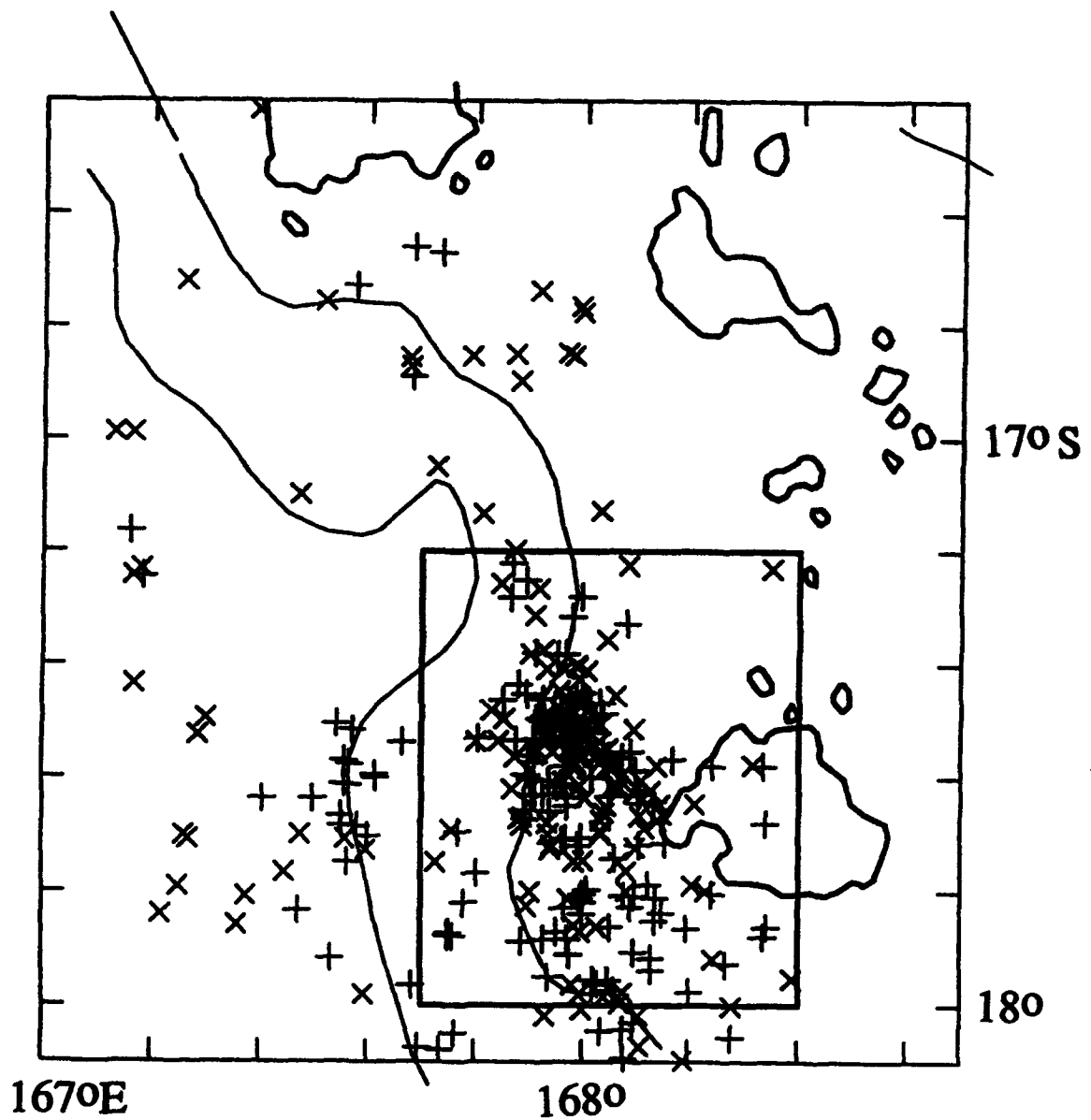


Figure 15. Map of preliminary locations of earthquakes recorded by OBS stations in this study. Crosses ("X") and pluses ("+") are events recorded in the first and second OBS deployments, respectively. Map only includes locations obtained using at least 4 P and 1 S observation and having an azimuthal gap of 330° or less. The box delineates the region mapped in Figure 16.

occurring near Efate (Figure 16). Each of locations utilized at least 4P and 2S arrivals and possessed an azimuthal gap smaller than 270°.

3. EVALUATION OF SOURCES OF LOCATION UNCERTAINTY

A. Background

In this course of the study we determined earthquake locations using a broad variety of fairly standard methods, i. e., for travel times, we utilized the IASPEI91 and J-B models as well as times determined from tracing rays in flat-earth models; for station corrections we employed both single-event relocation methods as well as JHD and JED methods. The events themselves included shallow earthquakes recorded only by teleseismic stations, shallow earthquakes recorded only by local stations, and intermediate focus earthquakes recorded by both regional and teleseismic stations. For this study the flexible character of the TexFlex relocation program (Frohlich, 1993) was essential, as it allowed us to carry out most of the different relocations above simply by changing a single parameter in the data input files.

The objective in this section is to compare and evaluate the locations in different geographic regions to reach some overall conclusions about the sources of location uncertainties for events located using travel-time based methods. For this study we have three different ways to evaluate the quality of locations; these are:

- 1) Dependence of the variance of travel time residuals on the method of location and the selection of data (Table 4);
- 2) Difference in geographic locations as determined by independent agencies (Figures 6 and 11); and
- 3) Dependence of volume of the bounding polyhedron on the method of location and selection of data (Table 6 and Figure 10).

For the purposes of discussion of travel time variances, we shall assume that location uncertainties contribute approximately additively to the variance V_{tot} of travel time residuals for groups of locations determined by a single-event method. It is reasonable to assume that errors contribute additively as the square of residuals since all the location algorithms used are least-squares algorithms, i.e., they minimize the sum of squares of residuals.

Thus, to formulate a crude model of the location uncertainty we posit that:

$$V_{tot} = V_{data} + V_{stations} + V_{velocity-model} + V_{other} = (RMS)^2$$

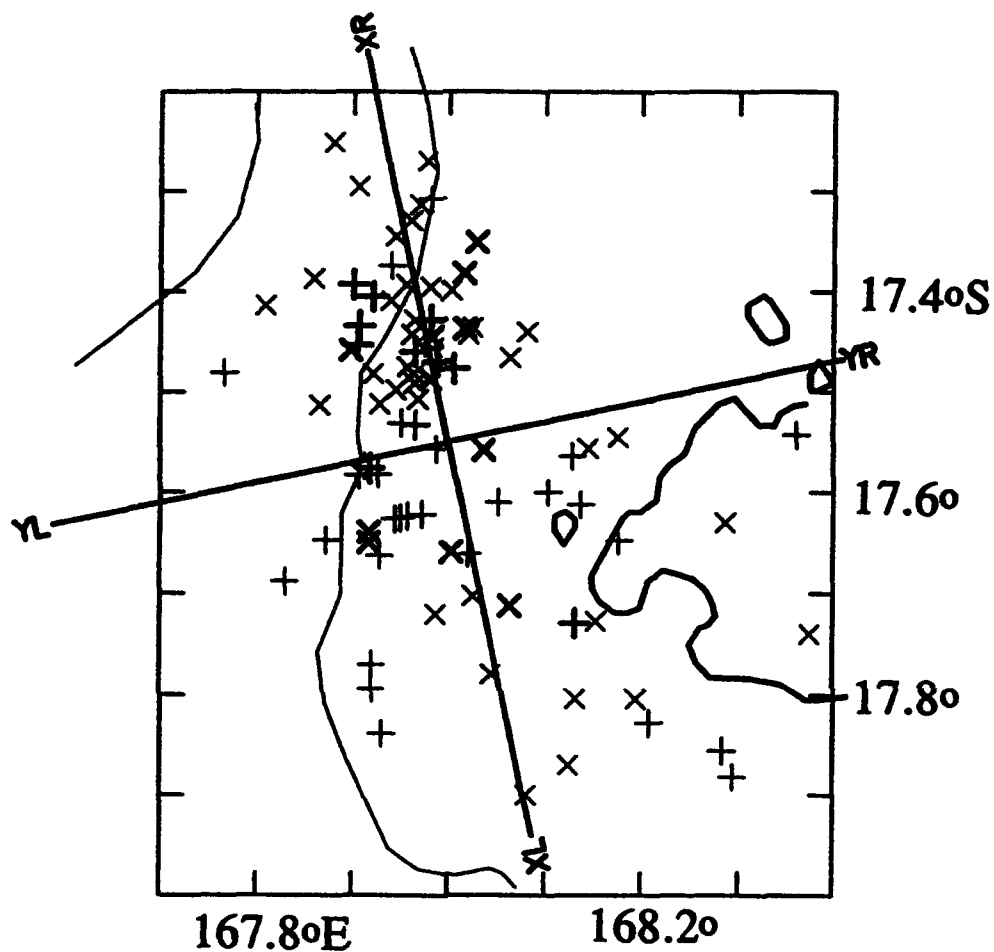


Figure 16. Map of relocations for earthquakes near Efate. Crosses and pluses are as in Figure 15; heavy dark symbols are for 21 especially well-recorded earthquakes used to determine station corrections; lighter symbols are 71 moderately well-recorded events (see text). Lines marked "XL - XR" and "YL - YR" show locations of cross sections in Figure 17.

and estimate the relative sizes of each of the components of V_{tot} for the different location regimes. Here, V_{data} represents variance attributable to incorrect identification of phase arrivals or misreading phase arrivals; $V_{stations}$ represents variance attributable to near-station structure, or to path effects which strongly influence a single station; $V_{velocity-model}$ represents variance which affects all stations, and is attributable to choosing an inappropriate model for relocating the group of events; and V_{other} represents other sources of variance, or sources of variance that should be assigned to V_{data} , $V_{stations}$, or $V_{velocity-model}$ but which our analysis is unable to detect. While this model clearly does not account properly for all sources of error (e.g., it wrongly suggests that earthquake locations with zero residuals possess no location error), it is a useful construct for comparing uncertainties of groups of earthquake locations determined by a variety of different least-squares methods.

B. Misreading or Incorrect Identification of Phase Arrivals

One approach to estimating the variance V_{data} due to misreading or mispicking of phase data is to evaluate the differences in phase arrival times as picked independently by different readers. If we imagine a hypothetical situation where both the velocity model used to determine travel times and the station corrections were known exactly, then, the only source of variance would be misidentification of phases or picking errors. If two readers each pick times so that their pick errors have variance V_1 and V_2 respectively, then the difference in picks will have variance $V_1 + V_2$. Thus, if $D_{mean-square}$ is the mean square difference in travel time picks for two independent readers, and if $V_1 = V_2$, an approximation for the true variance would be:

$$V_{data} = D_{mean-square} / 2$$

Since similarly trained readers evaluating the same data are likely to make the same errors in reading or phase identification, half the mean square difference in picks (Table 3) probably underestimates the true size of V_{data} .

For Macquarie, $D_{mean-square}$ is 0.60 sec^2 , suggesting that V_{data} is at least 0.30 sec^2 or greater. For Bucaramanga, $D_{mean-square}$ is 0.44 sec^2 suggesting that V_{data} is at least 0.22 sec^2 or greater. For Efate, $D_{mean-square}$ is 0.09 sec^2 , suggesting that V_{data} is 0.045 sec^2 or larger. Represented as fractions of V_{tot} as estimated from the single-event variance, these estimates of V_{data} represents 24% of V_{tot} in Macquarie, 4% in Bucaramanga, and 20% in Efate (Table 7).

C. Near-Station or Station-Path Effects

Since the JED and JHD methods were specifically designed to adjust event relocations for station-assignable sources of location uncertainty, a good estimate of the size of V_{stations} is the difference in variance for event groups relocated with single-event and with JED or JHD methods. For Macquarie Ridge the difference (Table 4) in variance between single-event and JED relocations was 0.42 sec^2 for the IASPEI91 model, or 33% of the total variance of 1.25 sec^2 (Table 7). For the J-B model the difference was 0.64 sec^2 , or 47% of the total variance of 1.35 sec^2 . For Bucaramanga, the IASPEI91 variance difference was about 4.50 sec^2 , or 90% of the total variance when the relocations were performed both with and without sP phases. Nearly all this variance difference was attributable to large systematic residuals at two stations, SJG and BHP. For Efate, Vanuatu, relocations using P and S phases at all stations, the variance difference was 0.17 sec^2 , or 73% of the total single-event variance of 0.23 sec^2 .

Table 7. Approximate percentage of travel time residual variance attributable to various sources in each of the three geographic regions studied. Sources are: V_{data} - variance due to misreading or mispicking phase arrival times; $V_{\text{station-path}}$ - variance due to near-station structure or path effects unique to a particular station; $V_{\text{velocity-model}}$ - variance attributable to incorrect choice of velocity model; V_{other} - estimate of remaining variance. Sum of estimates do not necessarily add up to 100% because all estimates are highly approximate.

Region	V_{data}	$V_{\text{station-path}}$	$V_{\text{velocity-model}}$	V_{other}
Macquarie Ridge	24%	30-50%	10%	16-36%
Bucaramanga	4%	90%	-	6%
Efate, Vanuatu	20%	73%	10%	<0%

Thus we conclude that the station-dependent contribution to location variance is of considerable importance. In situations such as Macquarie and Efate, Vanuatu where the degree of velocity inhomogeneity is apparently more-or-less "normal" it is still possible to reduce variance by 30-75% simply by determining station corrections. In situations such as Bucaramanga where there may be considerable lateral heterogeneity due to the presence of subducted lithosphere, the variance reduction may be 90% or more.

D. Velocity-Model Dependent Effects

To estimate the velocity-model-dependent sources of location variance $V_{\text{velocity-model}}$ we compare variances of event groups relocated the JED or JHD method using different velocity models. For Macquarie Ridge, the variance difference (Table 4) between IASPEI91 and J-B relocations was 0.12 sec^2 for JED relocations, corresponding to about 10% of the total single-event variance of 1.25 sec^2 (Table 7). For Bucaramanga, there was no variance difference for P-only J-B relocations using the J-B or IASPEI91 models. For Efate, Vanuatu, the variance difference between our preferred model and the simple layer-over-halfspace model was only 0.02 sec^2 , or about 10% of the total single-event variance of 0.23 sec^2 .

Thus, in all three regions the velocity-model dependent contribution to location variance of about 10% or less was smaller than either the station-dependent or the data-dependent contribution. However, we note that in the present study we were careful in all three geographic areas to evaluate only events for which we had reasonable azimuthal control. For events with poor azimuthal control the velocity-model-dependent location errors may be "hidden," since the least-squares method can then just adjust all the locations to accommodate differences in velocity model. Clearly, when azimuthal control is poor, a proper velocity model is essential for obtaining good locations.

E. Other Effects – Discussion

In this study V_{other} is the variance remaining after we have estimated V_{data} , V_{stations} , and $V_{\text{velocity-model}}$. For Macquarie Ridge, our approximate estimates above (Table 7) suggest that V_{other} is 16-36% of the V_{tot} , i.e., that either 16-36% of the variance is attributable to other sources, or that we have underestimated the importance of one or more of the sources of variance. For both Bucaramanga and Efate, the estimates of V_{other} are so small that they are indistinguishable from zero.

Incidentally, the size of differences in geographic location (Figures 6 and 11) for event locations reported by independent sources is roughly consistent with size of travel time variances. In particular, in both Macquarie and Bucaramanga the geographic differences were typically about 15 km, whereas the variances for single-event J-B locations were 1.35 sec^2 and 1.30 sec^2 , respectively. A variance of 1.3 sec corresponds to an RMS travel time residual of 1.15 sec. Now, $dT/d\Delta$ for phases between 30° and 90° ranges from 8.7 sec/degree to 4.6 sec/degree, or between

.08 sec/km and .04 sec/km. Thus, geographic differences of 15 km correspond roughly to travel time residuals of 0.6 sec to 1.2 sec.

However, the data concerning the effect of location method on the volume of bounding polyhedrons demonstrates that travel time variance itself gives an incomplete picture of location uncertainty. The Bucaramanga relocations, possessing reasonably good distribution of stations and phases which are generally impulsive, represent about as good accuracy as one can obtain by reading analog seismograms at teleseismic stations. Yet, in Bucaramanga the JHD relocations using P-phases only had a significantly smaller variance than those with P- and pP phases (0.28^2 sec compared to 0.48^2 sec, see Table 4, however, the bounding polyhedron volume was slightly smaller for the relocations with P- and pP (851 km^3 vs 687 km^3 see Table 5). Apparently the use of depth phases better constrains the hypocenters even though it increases the variance.

Also, these exercises demonstrate that adding more data can sometimes actually degrade the quality of locations. For example, in Bucaramanga the relocations that incorporated sP phases had both larger bounding polyhedrons ($1,176 \text{ km}^3$ vs 687 km^3) and larger variances (0.52 sec^2 vs 0.48 sec^2) than did locations using only P, PKP and pP.

Finally, the comparison of phase arrival picks read specifically for this study with those reported by the ISC (Table 3) indicated that when a strong phase existed and was reported, the time picks were in remarkably good agreement, usually within less than a half second. A more troubling result is that in a substantial fraction of cases either no phase was reported (15% and 26% for Macquarie and Bucaramanga), or a phase was reported at a time when we were unable to identify any significant arrival on the microfiche (24% and 16% for Macquarie and Bucaramanga). This suggests that blunders are a significant source of error in relocations using ISC reported phases. This will have only minor effects on research projects where there is ample data and the results effectively average all readings, such as determining the hypocenters of large, well-recorded earthquakes. However, these blunders can adversely affect research projects where there are few data, such as the relocation of small, poorly recorded earthquakes or explosions. Similarly, they could be crucial for projects where the results depend strongly on a few anomalous individual phase readings, such as travel time tomography in regions where there is significant lateral heterogeneity.

One implication of this study is that there are inherent weaknesses in any location method which relies solely on travel times. In particular, in specific cases we have demonstrated that whenever data is sparse large location errors are likely to arise from the effects of misread or

unread phase arrivals. Only when the number of observing stations is large will misread phases be identified as "outliers" in the pattern of residuals.

One possible promising approach that works even when the number of observing stations is small is to combine travel time analysis with waveform modeling. While excellent methods have been available for some time for modeling long period seismograms at teleseismic distances, there have recently been significant advances in the forward modeling of synthetic seismograms at regional, broadband stations (e.g., Zhao and Helmberger, 1991a; 1991b; 1993a; 1993b). Almost invariably forward modeling will constrain source depth more effectively than travel time analysis. Moreover, it is possible to locate an event if there is even one well-recorded digital, three-component record. While this is not always available, forward modeling to match available seismograms should place enough constraints on the locations so that one can identify blunders in phase arrival identification.

F. Summary and Conclusions

1. We have utilized a specially developed relocation program – TexFlex – to evaluate three groups of seismic events representing markedly different location scenarios; geographically these events are situated along the Macquarie Ridge; in the mantle beneath Bucaramanga, Colombia; and east of Efate, Vanuatu.

2. We here develop an approximate model to evaluate seismic location uncertainties by partitioning variance in travel time residuals between three sources: variance caused by errors in identifying and picking phases; variance which can be reduced by assigning station corrections; and variance produced by using an incomplete or inappropriate velocity model for relocation.

3. For events in all three geographic regions the largest identifiable source of variance is that associated with station corrections, representing 30-90% of the total variance for single-event relocations with no station correction.

4. The next largest source of variance was that associated with phase misidentification or mispicking, representing 4-24% of the total variance. For well-recorded phases there was remarkably little disagreement in the phase picks as determined by different readers, as the differences in arrival times averaged only 0.2-0.4 sec. A more troubling result was that for the teleseismic data, there were often phase arrivals reported at times where we could identify no arrival, or clear arrivals for which no phase was reported. This suggests that in practice picking

blunders, grossly misidentified phases, and unreported phases are more significant sources of error for teleseismic locations than is misreading of times for strong phases. Automatic picking of phase arrivals might help avoid these problems, although this may be unduly optimistic.

5. In this study the smallest source of variance was associated with an inappropriate velocity model. This source of variance was almost negligible for two of the three geographic regions, which were groups of events relocated using station corrections and with data having good azimuthal coverage. This suggests that if the objective is to determine good relative locations, when the azimuthal distribution of stations is good, it is often unnecessary to determine very detailed velocity models. If azimuthal distribution of stations is poor, accurate locations require a proper velocity model.

6. A previously developed way of evaluating location methods is to determine the volume of the smallest bounding polyhedron of groups of events known to originate from a localized source region – the assumption is then that smaller polyhedron volumes are associated with more accurate methods for determining relative locations. This approach reveals some inadequacies in the residual variance analysis.

7. Reducing residual variance is not always associated with smaller polyhedron volume. Moreover, adding more data sometimes actually degrades the locations, presumably when the additional data is of relatively poor quality. This implies that when data is sparse the optimal location strategy for a particular region should be to obtain data from a relatively few good stations (say, 6 stations), selected for high quality and for azimuthal coverage.

5. RESULTS OF REGIONAL/TECTONIC INTEREST

A. Macquarie Ridge

Two features of earthquakes in the Macquarie Ridge region are worthy of special note. First, the epicenters (Figure 3) seem to occur in several distinct clusters, possibly associated with the occurrence of a large earthquake. These clusters are separated by regions where activity is low or absent. In particular, these include:

- 1) A cluster occurring between about 46.5°S and 48°S, approximately in the region of the $m_b = 7.3$ thrust earthquake of 12 October, 1979;

- 2) A cluster occurring between about 49°S and 50°S, including the aftershock region of the $M_w = 7.6$ strike-slip earthquake of 25 May, 1981;
- 3) One or more clusters occurring between about 51°S and 55°S, including the aftershock region of the great $M_w = 8.1$ strike-slip earthquake of 23 May, 1989;
- 4) A cluster occurring between about 58.5°S and 60°S, near the epicenter of the $M_w = 7.4$ earthquake of 3 September, 1987.

An important question concerns whether the regions of low activity between the major clusters represent perennial regions of low activity; or whether instead they represent the sites of future great earthquakes. Although the locations of earthquakes prior to 1964 (Figure 1) are poorly determined, none with magnitudes larger than 7.2 or so have reported locations falling in the gaps between the clusters defined by the post-1964 data.

Another notable feature of Macquarie seismicity south of 47°S is there is little variability in focal mechanism type if one ignores principal axes that are poorly determined because they lie along the equatorial plane of earthquakes with large non-double-couple components. That is, the majority of well-determined mechanism axes (Figure 2) are nearly horizontal P axes, or nearly vertical B axes, as expected for strike-slip earthquakes. Thus the presence of a number of CMT with significant non-double-couple components seems to account for much of the alleged variability in mechanism type that had been previously noted by Frohlich et al. (1989).

An important unresolved question concerns the cause of the relatively large number of non-double-couple earthquakes observed in this region. In particular, are the non-double-couple components spurious, coming about merely because the region is so remote from most broadband digital seismic network stations? Or are the non-double-couple mechanisms real, related in some way to the complexity tectonics of this region, perhaps caused by the fact that the pole of rotation for Pacific-Australian motion is so close to the Macquarie Ridge?

B. Bucaramanga, Colombia

The present study is by no means the first to demonstrate the remarkable character of the earthquake activity comprising the Bucaramanga nest. Our relocations do find the dimension (~15-20 km) and volume (~700 km³) of the nest to be smaller than any previous study depending solely on teleseismic data. Presumably this is because of the care we have taken in using only data read by the author, and because we have relocated using a set of stations selected to give good azimuthal

coverage of the source region. However, these results are still considerably less localized than those found by Schneider et al. (1987) using data from a temporary local network.

One important difference between our results and those of Schneider et al. (1987) concerns the distribution of focal mechanisms for earthquakes within the Bucaramanga nest (Figure 8). When we consider only mechanisms determined from teleseismic observations, we find that the majority of the mechanisms possess T axes which dip eastward at about 45° , P axes which dip westward at about 45° , and B axes which are approximately north-south and horizontal. Thus, the resulting "sum" mechanism has one approximately horizontal nodal plane, and one approximately vertical nodal plane striking north-south.

In contrast, Schneider et al.'s (1987) mechanisms determined from local network data possess principal axes which are scattered over almost the entire focal sphere. We can only conclude that either there is a genuine difference between the mechanisms of large and small earthquakes within the nest, or that there was some unknown error in the data or method used to determine the mechanisms of the smaller events. In any case, if there was an error it may no longer be necessary to search for a physical explanation of the Bucaramanga nest which the extreme range of focal mechanisms noted by Schneider et al. (1987).

C. Efate, Vanuatu

Figure 16 and the accompanying cross sections (Figure 17) clearly demonstrate several important characteristics of the Efate nest. First, all but one of the hypocenters has a focal depth exceeding 25 km. Activity is absent at normal crustal depths, but quite intense between about 30 km and 45 km. The network geometry is not ideal for locating deeper events (e.g., see McLaren and Frohlich, 1985), but those visible presumably occur within an eastward-dipping Wadati-Benioff zone.

Second, the hypocenters making up the region of most intense activity between 30 km and 50 km depth form a diffuse cloud, which at first glance contains no obvious structure. However, more careful scrutiny suggests that this cloud includes a westward-dipping planar structure. Indeed, 50 of the 92 hypocenters in Figures 16 and 17 lie within 3 km of a planar surface having a westward dip of 33° and strike 12° W of N, delineated by arrows in Figure 18.

However, this planar surface is clearly not parallel to either nodal plane (Figure 18) for teleseismically determined centroid moment tensors (CMT) reported by Harvard for 38 earthquakes

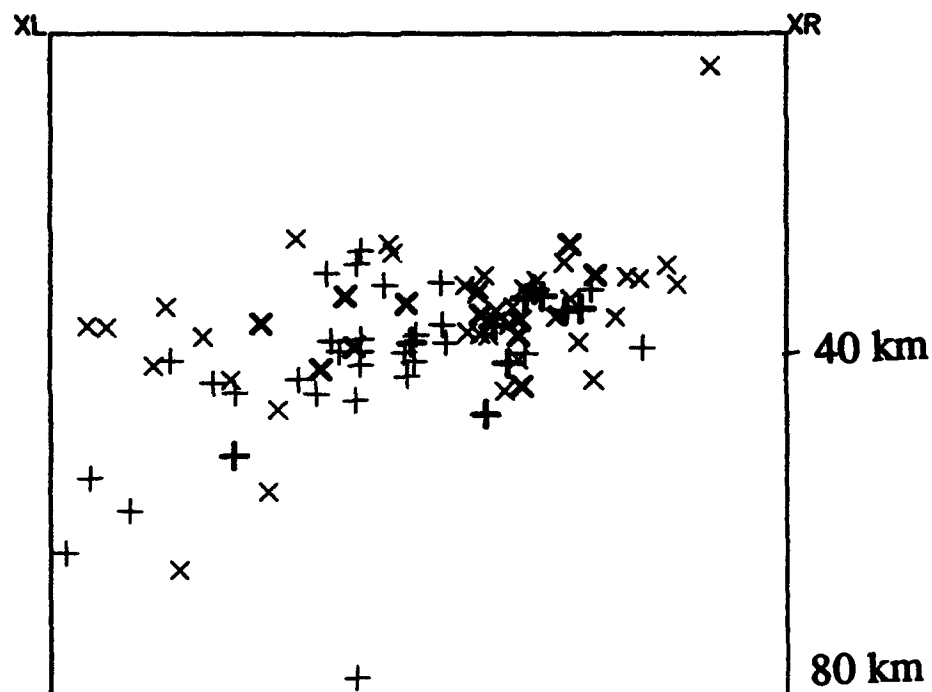
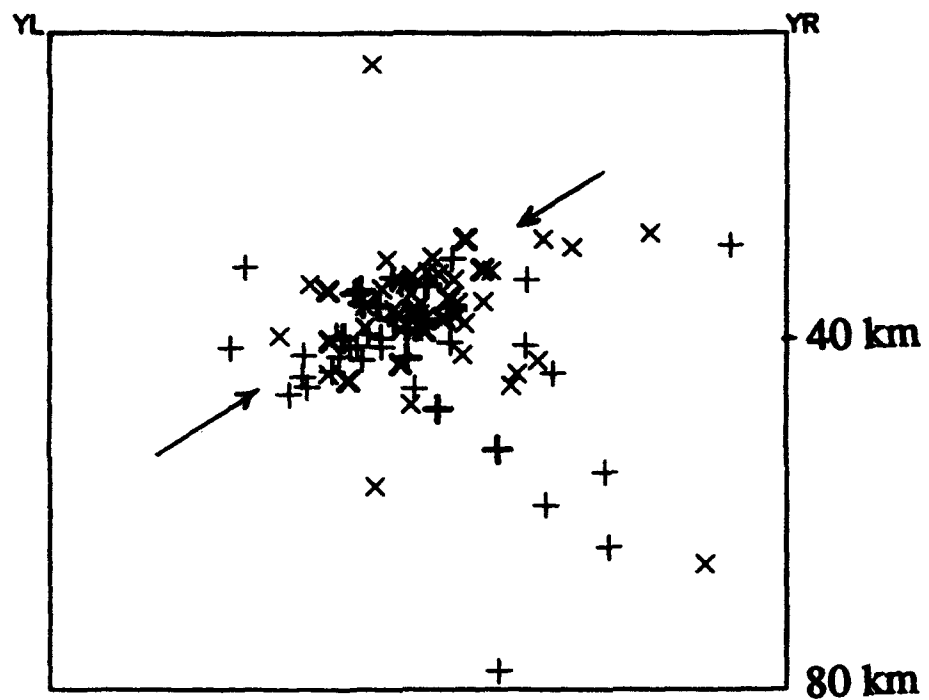


Figure 17. Cross sections of earthquake hypocenters mapped in Figure 16. Section marked "YL - YR" is a view looking approximately along the strike of the New Hebrides trench, while section marked "XL - XR" is an approximately perpendicular view. Arrows show orientation of planar surface situated within 3 km of 50 of the earthquakes in the section. Symbols are as in Figure 16.

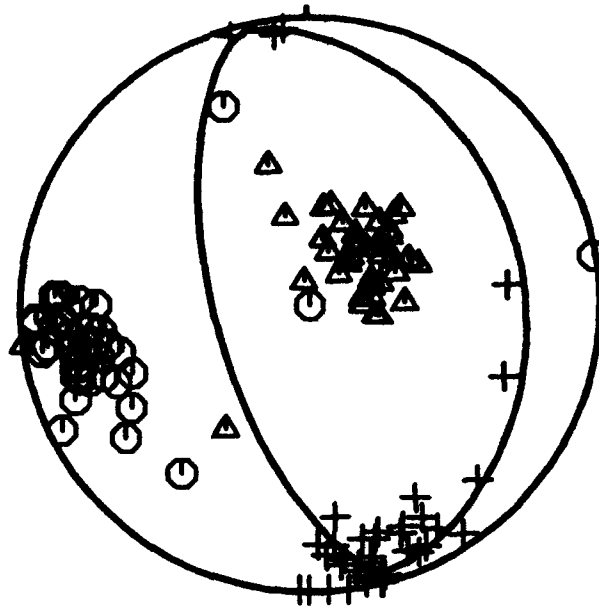


Figure 18. Composite focal plot of teleseismically determined CMT mechanisms for earthquakes which may occur within the Efate nest. Data are 38 Harvard CMT occurring since 1977 with epicenters occurring between 18.1°S and 17.0°S between 167.0°E and 168.1°E . Circles are P axes, triangles are T axes, and pluses are B axes for individual CMT, the heavy line shows the composite mechanism formed by adding together the individual moment tensors (see text).

occurring since 1977 in this area. These CMT are remarkable in that all but three are almost identical to one another. For the 38 CMT the seismic consistency C_S as defined by Frohlich and Apperson (1992) is 0.97, i.e., if we form the composite tensor by adding together the 38 individual CMT, the scalar moment of the composite tensor divided by the sum of individual scalar moments is 0.97. For the composite tensor the P axis has a dip of 18° , the T axis has a dip of about 72° and the B axis is horizontal with a strike of 14° W of N; thus, the nodal planes have dips of 63° westward and 27° eastward. Neither of these corresponds to the possible westward-dipping structure with a dip of 33° observable in Figure 17.

6. ACKNOWLEDGEMENTS

I am indebted to several individuals who contributed in essential ways to this study—they are: Millard Coffin, Shamita Das, Scott Davis, Katharine Kadinsky-Cade, Remy Louat, Yosio Nakamura, Paul Nyffeneger, and Dan Olson.

7. REFERENCES

- Abe, K., Magnitudes of large shallow earthquakes from 1904 to 1980, *Phys. Earth Planet. Int.*, 27, 72-92, 1981.
- Boyd, T.M. and J.A. Snoke, Error estimates in some commonly used location programs, *Earthquake Notes*, 55, 3-6, 1984.
- Chatelain, J.-L., B.L. Isacks, R.K. Cardwell, R. Prevot and M. Bevis, Patterns of seismicity associated with asperities in the central New Hebrides island arc, *J. Geophys. Res.*, 91, 12,497-12,519, 1986.
- Collot, J.Y. and M.A. Fisher, The collision zone between the north d'Entrecasteaux Ridge and the New Hebrides island arc, 1. Sea beam morphology and shallow structure, *J. Geophys. Res.*, 96, 4457-4478, 1991.
- Das, S., The Macquarie Ridge earthquake of 1989, *Geophys. J. Int.*, 115, 778-798, 1993.
- Dewey, J.W., Seismicity and tectonics of western Venezuela, *Bull. Seismol. Soc. Amer.*, 62, 1711-1752, 1972.

- Fisher, M.A., Y.Y. Collot and E.L. Geist, The collision zone Between the north d'Entrecasteaux Ridge and the New Hebrides Island Arc, 2. Structure from multichannel seismic data, *J. Geophys. Res.*, 96, 4479-4495, 1991.
- Flinn, E.A., Confidence regions and error determination for seismic event location, *Rev. Geophys.*, 3, 157-185, 1965.
- Frohlich, C., An efficient method for joint hypocenter determination for large groups of earthquakes, *Computers & Geosciences*, 5, 387-389, 1979.
- Frohlich, C., *An Integrated Approach to Seismic Event Location: I. Evaluating How Method of Location Affects the Volume of Groups of Hypocenters*, Phillips Laboratory Technical Report PL-TR-92-2323, ADA263211, Hanscom Air Force Base, Massachusetts, 1992.
- Frohlich, C., *Users Manual for TexFlex-0.5; The Texas Flexible, Practical Program Package for Locating Seismic Events*, University of Texas Institute for Geophysics Technical Report No. 128, 66 p., 1993.
- Frohlich, C. and K.D. Apperson, Earthquake focal mechanisms, moment tensor, and the consistency of seismic activity near plate boundaries, *Tectonics*, 11, 279-296, 1992.
- Frohlich, C., S. Billington, E. R. Engdahl and A. Malahoff, Detection and location of earthquakes in the central Aleutian subduction zone using island arc and ocean bottom seismograph stations, *J. Geophys. Res.*, 87, 6853-6864, 1982.
- Frohlich, C. and K. Kadinsky-Cade, An investigation of the practical limits of accuracy for relative seismic event locations, *Papers Presented at 15th Annual PL/DARPA Seismic Research Symposium*, PL-TR-93-2160, ADA271458, Vail, Colorado, 1993.
- Frohlich, C., R. Louat and Y. Nakamura, Earthquake activity in the southern Vanuatu arc recorded by the Texas digital OBS, *Mar. Geophys. Res.*, 12, 253-267, 1990.
- Frohlich, C., M.A. Riedesel and K.D. Apperson, Note concerning possible mechanisms for non-double-couple earthquake sources, *Geophys. Res. Lett.*, 16, 523-526, 1989.

Gutenberg, B. and C.F. Richter, *Seismicity of the Earth*, Princeton University Press, 1949.

Isacks, B. L., R.K. Cardwell, J.L. Chatelain, M. Barazangi, J.M. Marthelot, D. Chinn and R. Louat, Seismicity and tectonics of the central New Hebrides Island Arc, in *Earthquake Prediction: An International Review*, Maurice Ewing Ser., 4, edited by D. Simpson and P. Richards, 93-116, 1981.

Dewey, J.W., *Seismicity Studies with the Method of Joint Hypocenter Determination*, PhD Thesis, University of California at Berkeley, Berkeley, California, 1971.

Jeffreys, H. and K. Bullen, *Seismological Tables*, Grey Milne Trust, London, 1970.

Kennett, B. L. N., *IASPEI 1991 Seismological Tables*, Research School of Earth Sciences, Australian National University, Canberra, 1991.

Kennett, B.L.N. and E.R. Engdahl, Travel times for global earthquake location and phase identification, *Geophys. J. Int.*, 105, 429-465, 1991.

Louat, R., C. Frohlich, P. Charvis, Y. Hello, P. McPherson, Y. Nakamura and B. Pontoise, Etude d'une essaim seismes dans le Sud du Vanuatu (So. Pacifique) par un reseau de stations sismologiques sous-marines (OBS), *C. R. Acad. Sci., Paris, 309, Serie II*, 213-218, 1989.

McLaren, J.P. and C. Frohlich, Model calculations of regional network locations for earthquakes in subduction zones, *Bull. Seismol. Soc. Amer.*, 75, 397-413, 1985.

Nakamura, Y., P.L. Donoho, P.H. Roper and P.M. McPherson, Large-offset seismic suveying using ocean-bottom seismographs and air guns: Instrumentation and field techniques, *Geophys.*, 52, 1601-1611, 1987.

Pascal, G., B.L. Isacks, M. Barazangi and J. Dubois, Precise relocation of earthquakes and seismotectonics of the New Hebrides island arc, *J. Geophys. Res.*, 83, 4958-4973, 1978.

Pennington, W.D., Subduction of the eastern Panama basin and seismotectonics of northwestern South America, *J. Geophys. Res.*, 86, 10753-10770, 1981.

- Pennington, W.D., W.D. Mooney, R. van Hissenhoven, H. Meyer, J.E. Ramirez and R.P. Meyer, Results of a reconnaissance microearthquake survey of Bucaramanga, Colombia, *Geophys. Res. Lett.*, 6, 65-68, 1979.
- Prevot, R., S.W. Roecker, B.L. Isacks, and J.L. Chatelain, Mapping of low P wave velocity structures in the subducting plate of the central New Hebrides, Southwest Pacific, *J. Geophys. Res.*, 96, 19,825-19,842, 1991.
- Roecker, S.W., J.-L. Chatelain, B.L. Isacks and R., Prevot., Anomalous deep earthquakes beneath the New Hebrides Trench, *Bull. Seismol. Soc. Amer.*, 78, 1984-2007, 1988.
- Ruff, L.J., Special papers on the great Macquarie Ridge earthquake of 1989, ed. Ruff, L. J., *Geophys. Res. Lett.*, 17, 989-1024, 1990.
- Ruff, L.J., J.W. Given, C.O. Sanders and C.M. Sperber, Large earthquakes in the Macquarie Ridge complex: Transitional tectonics and subduction initiation, *Pure Appl. Geophys.*, 129, 71-129, 1989.
- Schneider, J.F., *The Intermediate-Depth Microearthquakes of the Bucaramanga Nest*, Colombia, Ph. D. dissertation, Univ. of Wisconsin, Madison, 233 pp., 1984.
- Schneider, J.J., W.D. Pennington and R.P. Meyer, Microseismicity and focal mechanisms of the intermediate-depth Bucaramanga Nest, Colombia, *J. Geophys. Res.*, 92, 13913-13926, 1987.
- Shih, X.R., R.P. Meyer and J.F. Schneider, An automated, analytical method to determine shear-wave splitting, *Tectonophys.*, 165, 271-278, 1989.
- Shih, X.R., R.P. Meyer and J.F. Schneider, Seismic anisotropy above a subducting plate, *Geology*, 19, 807-810, 1991.
- Shih, X.R., J.F. Schneider and R.P. Meyer, Polarities of P and S waves, and shear wave splitting observed from the Bucaramanga Nest, Colombia, *J. Geophys. Res.*, 96, 12069-12082, 1991.
- Taylor, F.W., B.L. Isacks, C. Jouannic, A.L. Bloom, and J. Dubois, Coseismic and Quaternary Vertical Movements, Santo and Malekula Islands, New Hebrides Islands Arc, *J. Geophys. Res.*, 85, 5367-5381, 1980.

- Taylor, F.W., C. Frohlich, J. Lecolle and M. Strecker, Analysis of partially emerged corals and reef terraces in the central Vanuatu arc: Comparison of contemporary coseismic and nonseismic with Quaternary vertical movements, *J. Geophys. Res.*, 92, 4905-4933, 1987.
- Trygvasson, E. and J.E. Lawson, The intermediate earthquake source near Bucaramanga, Colombia, *Bull. Seismol. Soc. Amer.*, 60, 269-276, 1970.
- Willemann, R.J. and C. Frohlich, Spatial patterns of aftershocks of deep focus earthquakes, *J. Geophys. Res.*, 92, 13927-13943, 1987.
- Zhao, L.-S. and D.V. Helmberger, Broadband modeling along a shield path, Harvard recording of the Saguenay earthquake, *Geophys. J. Int.*, 105, 301-312, 1991a.
- Zhao, L.-S. and D.V. Helmberger, Geophysical implications from relocations of Tibetan earthquakes: Hot Lithosphere, *Geophys. Res. Lett.*, 18, 2205-2208, 1991b.
- Zhao, L.-S. and D.V. Helmberger, Source retrieval from broadband regional seismograms: Hindu Kush region, *Phys. Earth Planet. Int.*, 78, 69-95, 1993a.
- Zhao, L.-S. and D.V. Helmberger, Regional moments, energy levels, and a new discriminant, *Bull. Seismol. Soc. Amer.*, (submitted) 1993b.

Prof. Thomas Ahrens
Seismological Lab, 252-21
Division of Geological & Planetary Sciences
California Institute of Technology
Pasadena, CA 91125

Dr. Robert Blandford
AFTAC/TT, Center for Seismic Studies
1300 North 17th Street
Suite 1450
Arlington, VA 22209-2308

Prof. Keiiti Aki
Center for Earth Sciences
University of Southern California
University Park
Los Angeles, CA 90089-0741

Dr. Stephen Bratt
ARPA/NMRO
3701 North Fairfax Drive
Arlington, VA 22203-1714

Prof. Shelton Alexander
Geosciences Department
403 Deike Building
The Pennsylvania State University
University Park, PA 16802

Dr. Lawrence Burdick
PO Box 80698
San Marino, CA 91118-8698

Prof. Charles B. Archambeau
CIRES
University of Colorado
Boulder, CO 80309

Dr. Robert Burridge
Schlumberger-Doll Research Center
Old Quarry Road
Ridgefield, CT 06877

Dr. Thomas C. Bache, Jr.
Science Applications Int'l Corp.
10260 Campus Point Drive
San Diego, CA 92121 (2 copies)

Dr. Jerry Carter
Center for Seismic Studies
1300 North 17th Street
Suite 1450
Arlington, VA 22209-2308

Prof. Muawia Barazangi
Institute for the Study of the Continent
Cornell University
Ithaca, NY 14853

Dr. Eric Chael
Division ~~9044~~ MS 0655
Sandia Laboratory
Albuquerque, NM 87185-0655

Dr. Jeff Barker
Department of Geological Sciences
State University of New York
at Binghamton
Vestal, NY 13901

Dr. Martin Chapman
Department of Geological Sciences
Virginia Polytechnical Institute
21044 Derring Hall
Blacksburg, VA 24061

Dr. Douglas R. Baumgardt
ENSCO, Inc
5400 Port Royal Road
Springfield, VA 22151-2388

Mr Robert Cockerham
Arms Control & Disarmament Agency
320 21st Street North West
Room 5741
Washington, DC 20451,

Dr. Susan Beck
Department of Geosciences
Building #77
University of Arizona
Tucson, AZ 85721

Prof. Vernon F. Cormier
Department of Geology & Geophysics
U-45, Room 207
University of Connecticut
Storrs, CT 06268

Dr. T.J. Bennett
S-CUBED
A Division of Maxwell Laboratories
11800 Sunrise Valley Drive, Suite 1212
Reston, VA 22091

Prof. Steven Day
Department of Geological Sciences
San Diego State University
San Diego, CA 92182

**US Dept of Energy
Recipient, IS-20, CA-033
Office of Resch & Development
1000 Independence Ave
Washington, DC 20585**

**Dr. Zoltan Der
ENSCO, Inc.
5400 Port Royal Road
Springfield, VA 22151-2388**

**Prof. Adam Dziewonski
Hoffman Laboratory, Harvard University
Dept. of Earth Atmos. & Planetary Sciences
20 Oxford Street
Cambridge, MA 02138**

**Prof. John Ebel
Department of Geology & Geophysics
Boston College
Chestnut Hill, MA 02167**

**Eric Fielding
SNEE Hall
INSTOC
Cornell University
Ithaca, NY 14853**

**Dr. Petr Firbas
Institute of Physics of the Earth
Masaryk University Brno
Jecna 29a
612 46 Brno, Czech Republic**

**Dr. Mark D. Fisk
Mission Research Corporation
735 State Street
P.O. Drawer 719
Santa Barbara, CA 93102**

**Prof Stanley Flatte
Applied Sciences Building
University of California, Santa Cruz
Santa Cruz, CA 95064**

**Prof. Donald Forsyth
Department of Geological Sciences
Brown University
Providence, RI 02912**

**Dr. Art Frankel
U.S. Geological Survey
922 National Center
Reston, VA 22092**

**Dr. Cliff Frolich
Institute of Geophysics
8701 North Mopac
Austin, TX 78759**

**Dr. Holly Given
IGPP, A-025
Scripps Institute of Oceanography
University of California, San Diego
La Jolla, CA 92093**

**Dr. Jeffrey W. Given
SAIC
10260 Campus Point Drive
San Diego, CA 92121**

**Dr. Dale Glover
Defense Intelligence Agency
ATTN: ODT-1B
Washington, DC 20301**

**Dan N. Hagedon
Pacific Northwest Laboratories
Battelle Boulevard
Richland, WA 99352**

**Dr. James Hannon
Lawrence Livermore National Laboratory
P.O. Box 808
L-205
Livermore, CA 94550**

**Prof. David G. Harkrider
Seismological Laboratory
Division of Geological & Planetary Sciences
California Institute of Technology
Pasadena, CA 91125**

**Prof. Danny Harvey
CIRES
University of Colorado
Boulder, CO 80309**

**Prof. Donald V. Helmberger
Seismological Laboratory
Division of Geological & Planetary Sciences
California Institute of Technology
Pasadena, CA 91125**

**Prof. Eugene Herrin
Institute for the Study of Earth and Man
Geophysical Laboratory
Southern Methodist University
Dallas, TX 75275**

Prof. Robert B. Herrmann
Department of Earth & Atmospheric Sciences
St. Louis University
St. Louis, MO 63156

Prof. Lane R. Johnson
Seismographic Station
University of California
Berkeley, CA 94720

Prof. Thomas H. Jordan
Department of Earth, Atmospheric &
Planetary Sciences
Massachusetts Institute of Technology
Cambridge, MA 02139

Prof. Alan Kafka
Department of Geology & Geophysics
Boston College
Chestnut Hill, MA 02167

Robert C. Kemerait
ENSCO, Inc.
445 Pineda Court
Melbourne, FL 32940

Dr. Karl Koch
Institute for the Study of Earth and Man
Geophysical Laboratory
Southern Methodist University
Dallas, Tx 75275

US Dept of Energy
Attn: Max Koontz, MM-20, GA-033
Office of Resch & Development
1000 Independence Ave, SW
Washington, DC 20585

Dr. Richard LaCoss
MIT Lincoln Laboratory, M-200B
P.O. Box 73
Lexington, MA 02173-0073

Dr. Fred K. Lamb
University of Illinois at Urbana-Champaign
Department of Physics
1110 West Green Street
Urbana, IL 61801

Prof. Charles A. Langston
Geosciences Department
403 Deike Building
The Pennsylvania State University
University Park, PA 16802

Jim Lawson, Chief Geophysicist
Oklahoma Geological Survey
Oklahoma Geophysical Observatory
P.O. Box 8
Leonard, OK 74043-0008

Prof. Thorne Lay
Institute of Tectonics
Earth Science Board
University of California, Santa Cruz
Santa Cruz, CA 95064

Dr. William Leith
U.S. Geological Survey
Mail Stop 928
Reston, VA 22092

Mr. James F. Lewkowicz
Phillips Laboratory/GPEH
29 Randolph Road
Hanscom AFB, MA 01731-3010(2 copies)

Mr. Alfred Lieberman
ACDA/VI-OA State Department Building
Room 5726
320-21st Street, NW
Washington, DC 20451

Prof. L. Timothy Long
School of Geophysical Sciences
Georgia Institute of Technology
Atlanta, GA 30332

Dr. Randolph Martin, III
New England Research, Inc.
76 Olcott Drive
White River Junction, VT 05001

Dr. Robert Masse
Denver Federal Building
Box 25046, Mail Stop 967
Denver, CO 80225

Dr. Gary McCartor
Department of Physics
Southern Methodist University
Dallas, TX 75275

Prof. Thomas V. McEvelly
Seismographic Station
University of California
Berkeley, CA 94720

Dr. Art McGarr
U.S. Geological Survey
Mail Stop 977
U.S. Geological Survey
Menlo Park, CA 94025

Dr. Keith L. McLaughlin
S-CUBED
A Division of Maxwell Laboratory
P.O. Box 1620
La Jolla, CA 92038-1620

Stephen Miller & Dr. Alexander Florence
SRI International
333 Ravenswood Avenue
Box AF 116
Menlo Park, CA 94025-3493

Prof. Bernard Minster
IGPP, A-025
Scripps Institute of Oceanography
University of California, San Diego
La Jolla, CA 92093

Prof. Brian J. Mitchell
Department of Earth & Atmospheric Sciences
St. Louis University
St. Louis, MO 63156

Mr. Jack Murphy
S-CUBED
A Division of Maxwell Laboratory
11800 Sunrise Valley Drive, Suite 1212
Reston, VA 22091 (2 Copies)

Dr. Keith K. Nakanishi
Lawrence Livermore National Laboratory
L-025
P.O. Box 808
Livermore, CA 94550

Prof. John A. Orcutt
IGPP, A-025
Scripps Institute of Oceanography
University of California, San Diego
La Jolla, CA 92093

Prof. Jeffrey Park
Kline Geology Laboratory
P.O. Box 6666
New Haven, CT 06511-8130

Dr. Howard Patton
Lawrence Livermore National Laboratory
L-025
P.O. Box 808
Livermore, CA 94550

Dr. Frank Pilotte
HQ AFTAC/TT
1030 South Highway A1A
Patrick AFB, FL 32925-3002

Dr. Jay J. Pulli
Radix Systems, Inc.
201 Perry Parkway
Gaithersburg, MD 20877

Dr. Robert Reinke
ATTN: FCTVTD
Field Command
Defense Nuclear Agency
Kirtland AFB, NM 87115

Prof. Paul G. Richards
Lamont-Doherty Geological Observatory
of Columbia University
Palisades, NY 10964

Mr. Wilmer Rivers
Teledyne Geotech
314 Montgomery Street
Alexandria, VA 22314

Dr. Alan S. Ryall, Jr.
ARPA/NMRO
3701 North Fairfax Drive
Arlington, VA 22203-1714

Dr. Richard Sailor
TASC, Inc.
55 Walkers Brook Drive
Reading, MA 01867

Prof. Charles G. Sammis
Center for Earth Sciences
University of Southern California
University Park
Los Angeles, CA 90089-0741

Prof. Christopher H. Scholz
Lamont-Doherty Geological Observatory
of Columbia University
Palisades, NY 10964

Dr. Susan Schwartz
Institute of Tectonics
1156 High Street
Santa Cruz, CA 95064

Secretary of the Air Force
(SAFRD)
Washington, DC 20330

Office of the Secretary of Defense
DDR&E
Washington, DC 20330

Thomas J. Sereno, Jr.
Science Application Int'l Corp.
10260 Campus Point Drive
San Diego, CA 92121

Dr. Michael Shore
Defense Nuclear Agency/SPSS
6801 Telegraph Road
Alexandria, VA 22310

Dr. Robert Shumway
University of California Davis
Division of Statistics
Davis, CA 95616

Dr. Matthew Sibol
Virginia Tech
Seismological Observatory
4044 Derring Hall
Blacksburg, VA 24061-0420

Prof. David G. Simpson
IRIS, Inc.
1616 North Fort Myer Drive
Suite 1050
Arlington, VA 22209

Donald L. Springer
Lawrence Livermore National Laboratory
L-025
P.O. Box 808
Livermore, CA 94550

Dr. Jeffrey Stevens
S-CUBED
A Division of Maxwell Laboratory
P.O. Box 1620
La Jolla, CA 92038-1620

Lt. Col. Jim Stobie
ATTN: AFOSR/NL
110 Duncan Avenue
Bolling AFB
Washington, DC 20332-0001

Brian Stump
Los Alamos National Laboratory
KES-3, Mail Stop C335
Los Alamos, NM 87545

Prof. Jeremiah Sullivan
University of Illinois at Urbana-Champaign
Department of Physics
1110 West Green Street
Urbana, IL 61801

Prof. L. Sykes
Lamont-Doherty Geological Observatory
of Columbia University
Palisades, NY 10964

Dr. David Taylor
ENSCO, Inc.
445 Pineda Court
Melbourne, FL 32940

Dr. Steven R. Taylor
Los Alamos National Laboratory
P.O. Box 1663
Mail Stop C335
Los Alamos, NM 87545

Prof. Clifford Thurber
University of Wisconsin-Madison
Department of Geology & Geophysics
1215 West Dayton Street
Madison, WI 53706

Prof. M. Nafi Toksoz
Earth Resources Lab
Massachusetts Institute of Technology
42 Carleton Street
Cambridge, MA 02142

Dr. Larry Turnbull
CIA-OSWR/NED
Washington, DC 20505

Dr. Gregory van der Vink
IRIS, Inc.
1616 North Fort Myer Drive
Suite 1050
Arlington, VA 22209

Dr. Karl Veith
EG&G
5211 Auth Road
Suite 240
Suitland, MD 20746

Prof. Terry C. Wallace
Department of Geosciences
Building #77
University of Arizona
Tucson, AZ 85721

Dr. Thomas Weaver
Los Alamos National Laboratory
P.O. Box 1663
Mail Stop C335
Los Alamos, NM 87545

Dr. William Wortman
Mission Research Corporation
8560 Cinderbed Road
Suite 700
Newington, VA 22122

Prof. Francis T. Wu
Department of Geological Sciences
State University of New York
at Binghamton
Vestal, NY 13901

Prof Ru-Shan Wu
University of California, Santa Cruz
Earth Sciences Department
Santa Cruz
CA 95064

ARPA, OASB/Library
3701 North Fairfax Drive
Arlington, VA 22203-1714

HQ DNA
ATTN: Technical Library
Washington, DC 20305

Defense Intelligence Agency
Directorate for Scientific & Technical Intelligence
ATTN: DTIB
Washington, DC 20340-6158

Defense Technical Information Center
Cameron Station
Alexandria, VA 22314 (2 Copies)

TACTEC
Battelle Memorial Institute
505 King Avenue
Columbus, OH 43201 (Final Report)

Phillips Laboratory
ATTN: XPG
29 Randolph Road
Hanscom AFB, MA 01731-3010

Phillips Laboratory
ATTN: GPE
29 Randolph Road
Hanscom AFB, MA 01731-3010

Phillips Laboratory
ATTN: TSML
5 Wright Street
Hanscom AFB, MA 01731-3004

Phillips Laboratory
ATTN: PL/SUL
3550 Aberdeen Ave SE
Kirtland, NM 87117-5776 (2 copies)

Dr. Michel Bouchon
I.R.I.G.M.-B.P. 68
38402 St. Martin D'Herès
Cedex, FRANCE

Dr. Michel Campillo
Observatoire de Grenoble
I.R.I.G.M.-B.P. 53
38041 Grenoble, FRANCE

Dr. Kin Yip Chun
Geophysics Division
Physics Department
University of Toronto
Ontario, CANADA

Prof. Hans-Peter Harjes
Institute for Geophysics
Ruhr University/Bochum
P.O. Box 102148
4630 Bochum 1, GERMANY

Prof. Eystein Husebye
NTNF/NORSAR
P.O. Box 51
N-2007 Kjeller, NORWAY

David Jepsen
Acting Head, Nuclear Monitoring Section
Bureau of Mineral Resources
Geology and Geophysics
G.P.O. Box 378, Canberra, AUSTRALIA

Ms. Eva Johannisson
Senior Research Officer
FOA
S-172 90 Sundbyberg, SWEDEN

Dr. Peter Marshall
Procurement Executive
Ministry of Defense
Blacknest, Brimpton
Reading FG7-FRS, UNITED KINGDOM

Dr. Bernard Massinon, Dr. Pierre Mechler
Societe Radiomana
27 rue Claude Bernard
75005 Paris, FRANCE (2 Copies)

Dr. Svein Mykkeltveit
NTNT/NORSAR
P.O. Box 51
N-2007 Kjeller, NORWAY (3 Copies)

Prof. Keith Priestley
University of Cambridge
Bullard Labs, Dept. of Earth Sciences
Madingley Rise, Madingley Road
Cambridge CB3 0EZ, ENGLAND

Dr. Jorg Schlittenhardt
Federal Institute for Geosciences & Nat'l Res.
Postfach 510153
D-30631 Hannover, GERMANY

Dr. Johannes Schweitzer
Institute of Geophysics
Ruhr University/Bochum
P.O. Box 1102148
4360 Bochum 1, GERMANY

Trust & Verify
VERTIC
Carrara House
20 Embankment Place
London WC2N 6NN, ENGLAND